Topological constraints on quasicrystal transformations

David M. Frenkel, Christopher L. Henley, and Eric D. Siggia
Laboratory of Atomic and Solid State Physics, Cornell University, Clark Hall, Ithaca, New York 14853-2501
(Received 7 April 1986)

The notion of a perfect crystal in d-dimensional physical space may be generalized to the "deterministic" quasicrystal generated by a cut by a d-dimensional "physical" plane through a periodic array of $(D-d)$-dimensional hypersurfaces in a D-dimensional space. (The quasicrystal tilings generated by projection from a D-dimensional lattice are a special case.) When these surfaces are smooth, and we impose a noncrystallographic symmetry (e.g., a fivefold axis), then they must intersect, which is unphysical. We explore the topology of the transformations induced on these structures by transverse displacements of the physical plane, which correspond to the phase degree of freedom in incommensurate structures. For the projected structures, the atoms undergo a nontrivial permutation when the physical plane is transported in a small closed loop about a vertex of the D-dimensional lattice. We see no way to build a deterministic model for the quasicrystals of physical interest in which the individual atoms move continuously in response to transverse displacements of the physical plane. Thus the conventional spontaneously broken continuous symmetry arguments for a hydrodynamic "phason" mode no longer apply. We suggest that real quasicrystals are nondeterministic and speculate about possible glassy properties of these materials.

I. INTRODUCTION

The discovery of alloys with electron diffraction patterns with icosahedral[1] or decagonal[2] symmetry led immediately to attempts to model their structure. The spots are sufficiently sharp to suggest that an ideal sample would have Bragg (δ-function) spots, indicating long-range order; but ordinary periodic crystalline order is ruled out by the existence of noncrystallographic fivefold axes. The apparent paradox was resolved by the exhibition of mathematical structures, known as Penrose tilings, which have noncrystallographic symmetries but have δ-function Fourier transforms.[3,4] These structures are almost periodic[5] and incommensurate. Another geometrical model with the same symmetries was given by a sum of density waves with wave vectors in icosahedrally symmetric directions.[6–10]

Incommensurate structures are well studied,[11,12] but the only examples known before the discovery of quasicrystals were ordinary periodic crystals with an incommensurate modulation superimposed. The atomic structure of such crystals (in d dimensions) may be conveniently represented by a cut through a D-dimensional space, where $d_\perp = D - d$ is the number of independent incommensurate modulation vectors.[13,14] The case $d = d_\perp = 1$ is realized by the Frenkel-Kontorova[15] model, a chain of atoms connected by springs which have a preferred spacing which competes with an external pinning potential whose minima have a different, incommensurate spacing.

In this paper we do not consider potentials, but only the geometric properties which any such structure must satisfy. We start from the fact that quasicrystals can also be represented by a density in a D-dimensional space (see Appendix A). In particular, the analog of a perfect (disorder-free) crystal consists of a set of $d_\perp$-dimensional hypersurfaces periodic with respect to the D-lattice.[16–21] It is tempting to assume that the atomic surfaces are smooth and nonintersecting. Both properties are realized by the solutions to the Frenkel-Kontorova model. However, if the atomic surface possesses a noncrystallographic symmetry (e.g., a fivefold axis), the smoothness assumption is untenable. We therefore say that a smooth deterministic quasicrystal cannot exist.

We examine these pathologies in more detail through the *transformations* induced on the atomic positions by displacements of the physical plane. More precisely, resolve all D-dimensional vectors, $\mathbf{x}$, into components $\mathbf{x}^{\parallel}$, parallel to the physical plane, and $\mathbf{x}^{\perp}$, perpendicular to it. The physical plane is defined by its intercept $\mathbf{x}_0^{\perp}$, which therefore specifies a particular pattern of atoms. Displacements of $\mathbf{x}_0^{\perp}$ generate the desired transformations. The physical assumptions mentioned above imply that atoms should move continuously with $\mathbf{x}_0^{\perp}$, and never get too close.

The projection construction[5–7,22–26] has the unphysical feature that atoms can jump under displacements of $\mathbf{x}_0^{\perp}$, though there is no ambiguity of keeping track of which atom goes where. The "pathology" mentioned above now manifests itself as a nontrivial permutation in the atomic pattern when $\mathbf{x}_0^{\perp}$ is moved around a small closed loop.

These permutations are not an artifact of projection. Indeed, we show how to smooth out the atomic surface defined by projection so that atoms move continuously. The permutations remain, and in addition the atomic surfaces branch. That is, atoms are allowed to come arbitrarily close and there are only a finite number of disconnected atomic surfaces.

The absence of a "deterministic" algorithm for building a quasicrystal has important implications for the allowed hydrodynamic modes.[6,7,9,10,16,27,28] If the orientation of the physical plane is incommensurate, then all atomic patterns should have the same energy for reasonable poten-

tials since the frequencies of local arrangements of atoms are independent of $\mathbf{x}_0^\perp$ (Ref. 4). One would suppose that displacements in $\mathbf{x}_0^\perp$ are a symmetry, and indeed the density wave models mentioned above provide a concrete realization of this property. The corresponding Goldstone modes are called phasons.[11,12] Before one can hope to extend this symmetry to a more realistic energy involving the atomic positions, one must have the atomic positions defined so that they vary smoothly with $\mathbf{x}_0^\perp$ and do not overlap. The symmetry, acting on configuration space, must be continuous before one can exploit it dynamically. We see no way to define atomic positions deterministically so they vary continuously with $\mathbf{x}_0^\perp$. While the usual broken symmetry arguments do not suffice at the atomic level to guarantee the existence of soft modes, we cannot preclude their presence in some more coarse grained model. Should soft modes associated with $\mathbf{x}_0^\perp$ exist in a density wave description, the underlying atomic displacements will be nondeterministic. That is, there will be no smooth atomic surface that one can specify within a single hypercube, which would define the atomic positions everywhere. We believe some degree of disorder is unavoidably present in these structures and speculate about its possible form in the Conclusion.

An outline of the paper is as follows. In Sec. II we discuss in some detail the simple case of $D=3$, $d=1$ ($3\rightarrow 1$). This example has all the features of the $2\rightarrow 1$ case, including phasons, yet permits one to introduce several constructs that will be useful later on.

In Sec. III we formally define several of the terms we have used casually above and then prove that a fivefold axis contradicts the properties (described in detail in that section) we assumed for the atomic surface.

Section IV analyzes the $4\rightarrow 2$ case since it contains all the complexity of the higher-dimensional examples of physical interest but is much easier to visualize. Both the structure defined by projection and its smoothed version are explored. In Sec. V both these constructions are carried over to the $5\rightarrow 2$ and $6\rightarrow 3$ examples of physical interest.

In the Conclusion we comment on earlier discussion of the phason modes in relation to our findings, on the distinction between incommensurately modulated crystals and quasicrystals, and other technical points. The connection between symmetry of the diffraction pattern and the symmetry of the hyperspace is outlined in Appendix A. Appendix B proves several counting formulas used in Sec. V. Appendix C elaborates on the permutation group induced by small displacements of $\mathbf{x}_0^\perp$ around a vertex in the $5\rightarrow 2$ case.

II. A SIMPLE EXAMPLE

The $3\rightarrow 1$ projection is still easily visualized, yet permits one to illustrate several desirable by-products of the projection technique that are either absent or too trivial in the $2\rightarrow 1$ case. The "physical plane" is just a line that has irrational direction cosines. We project onto this line the center of any cube that the line enters.[29] One thereby marks off on the line a quasiperiodic series of points with three fundamental frequencies.

We would like to construct a family of 2D surfaces, which we call *atomic surfaces,* such that their intersections with the physical line form the same set of points as obtained by projecting the center of each cube the line enters.

To see if the physical line enters a particular cube, project that cube onto the two-dimensional *normal plane,* perpendicular to the physical line. The "shadow" thus formed is a hexagon whose opposite sides are parallel,[30] and each of which is the projection of a specific edge of the cube. We will call such edges of the cube *silhouetting* edges. The physical line is fixed once we specify its intercept with the normal plane, $\mathbf{x}_0^\perp$. Clearly, the line will enter the cube only if the cube's shadow contains $\mathbf{x}_0^\perp$.

Now, in each cube, passing through its center, we place a hexagonal piece of 2D plane (which we call a *patch)* oriented normal to the physical line and whose projection into the normal plane coincides with the cube's shadow. Manifestly, the physical line intersects this piece of surface only if it enters the cube, and the point of intersection is obviously the point the cube's center gets projected into. Figure 1(a) depicts a similar construction for the $2\rightarrow 1$ case, which is simpler to draw.

The set of all patches constructed above form a desired atomic surface. However, we would like to connect the patches from various cubes into a family of extended atomic surfaces. To see how it can be done, consider moving $\mathbf{x}_0^\perp$, which corresponds to moving the physical line. Viewed on the normal plane, it must exit a particular hexagon through one of its edges and enter another one right away. Back in three dimensions, the new cube is adjacent to the old one along the 1-edge whose projection is the common edge of the two hexagons. When, for example, the direction cosines of the physical line are all positive, the new cube is the result of shifting the old one by a vector from the set $\Gamma=\{\pm(1,-1,0), \pm(1,0,-1),\pm(0,1,-1)\}$ in which only two vectors are linearly independent. These vectors, if drawn from the cube center, just point toward the edges shared by the two cubes, which are seen to coincide with the silhouetting edges. Continuity in the normal space unambiguously defines how the cubes must be linked. The sole possible ambiguity occurs at the vertices of the hexagons which can be hit at most once for an irrationally oriented line.

A piece of plane parallel to the physical direction is then inserted along the common edges of patches that are to be linked. We term these linking planes *steps* and they complete the construction of a family of atomic surfaces that are equivalent to projection. Figure 1 shows how our definitions would look in the $2\rightarrow 1$ case. Clearly all surfaces in the family differ by only a displacement.

We can smooth out this surface to eliminate the steps without altering its topology or periodicity.[16–18,21] Redefine the surface patch associated with each cube to be the pencil of rays from the cube center to the six silhouetting edges (Fig. 2). They are precisely the edges shared by contiguous cubes linked together into a single atomic surface. The steps are no longer necessary and the new surface passes smoothly from cube to cube (Fig. 3).

It will be necessary, for what follows, to make one additional modification to our smoothed atomic surface. As

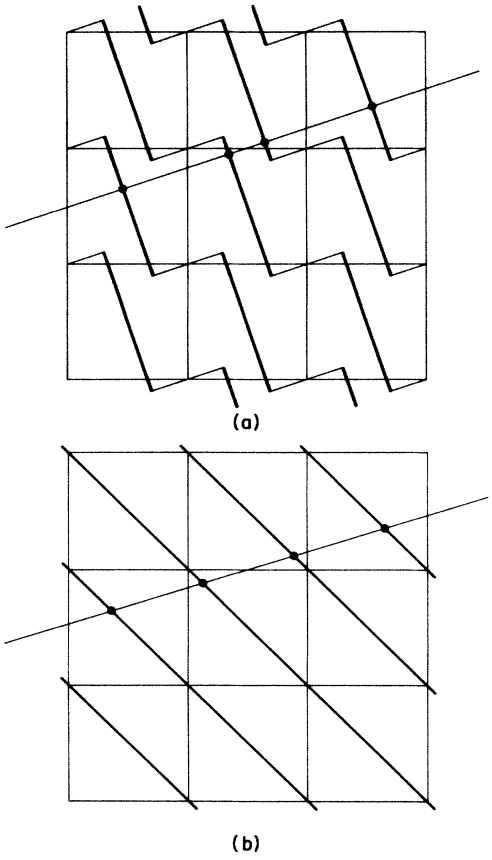

FIG. 1. Stepped atomic surface and its smoothed out version for the $2\rightarrow 1$ projection. (a) A physical line intersects a series of stepped lines in the figure, which defines "atoms" on the physical line (represented by dots). This particular choice of stepped lines is equivalent to projecting the center of each cube the physical line enters. Note the linking "steps," represented by thinner lines, that are parallel to the physical line. They are really superfluous for defining projection, but are useful for defining connectedness of the infinite surfaces. In (b) the steps are smoothed out and the atoms no longer jump under displacements of the physical line.

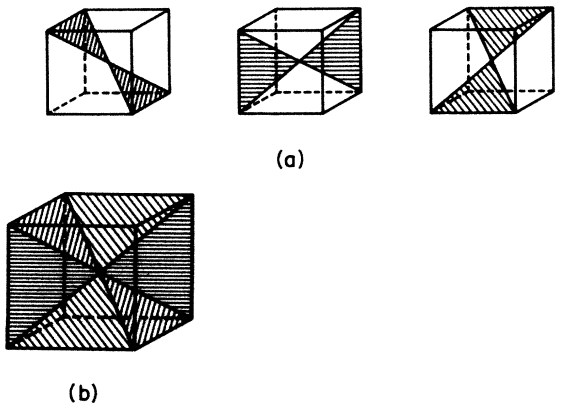

FIG. 2. Construction of the smooth atomic surface within a single cube for the $3\rightarrow 1$ projection. The physical line has positive direction cosines. The pairs of edges in (a) fall on opposite sides of the hexagon when the entire cube is projected onto the normal plane. Sketch (b) shows the pieces of the surface assembled.

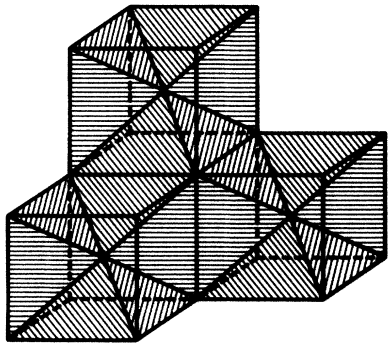

FIG. 3. A portion of the extended atomic surface for the $3\rightarrow 1$ projection. Note that the cube centers are related by the modout vectors $\Gamma=\{(1,-1,0),(1,0,-1),(0,1,-1)\}$. If the lower left center is at $(\frac{1}{2},\frac{1}{2},\frac{1}{2})$, then the vertex (0,1,1) is shared by the surface through the next layer of cubes with centers $(\frac{1}{2},\frac{1}{2},\frac{3}{2})$, $(\frac{1}{2},\frac{3}{2},\frac{1}{2})$, $(-\frac{1}{2},\frac{3}{2},\frac{3}{2})$, etc. *Local* surgery is sufficient to separate the surfaces, as explained in the text.

just defined, successive surfaces touch at isolated points. That is, certain vertices are shared by cube edges which belong to different surfaces. It is clear that by doing a *local* surgery near these vertices, we can maintain a nonzero minimum spacing between the surfaces while not violating the condition that they each have a 1:1 projection onto the normal plane.

For the $3\rightarrow 1$ projection, we evidently can make three statements.

(a) The shadowing hexagons tile the normal plane.

(b) The 3-cubes may be partitioned into disjoint classes, each of which projects 1:1 onto the normal plane and yields a hexagonal tiling.

(c) The classes in (b) may be defined by an equivalence relation which places two cubes in the same class if and only if their centers are related by integer linear combinations of (any two) vectors from the set Γ above.

To summarize, the physical line hits precisely one cube in each class and no classes are omitted. Equivalently, the atomic surfaces are disjoint and each has a 1:1 projection onto the normal plane. The positions of atoms vary smoothly with $\mathbf{x}_0^{\perp}$ and respect a minimum separation.

III. SYMMETRY CONSIDERATIONS

A. Definitions and general considerations

The considerations in the Introduction and our previous example allow us to state a series of physical conditions that any scheme for enumerating the atomic positions in a perfect quasicrystal should have. In the $3\rightarrow 1$ case the smooth atomic surface derived from projection satisfies all those conditions. In higher dimensions one or another of these conditions will be violated by any atomic surface, so it will facilitate the discussion to state them explicitly.

Condition (0): Determinism. The atomic positions are defined by intersecting a d-dimensional physical plane, whose precise location is determined by $\mathbf{x}_0^{\perp}$, its point of in-

tersection with a normal plane, with a D-dimensional surface.

Condition (1): Periodicity. The atomic surface is periodic in $D > d$ dimensions.

Condition (2): Conservation of atoms. Under changes in $\mathbf{x}_0^\perp$, atoms are never created or destroyed.

Condition (3): Smoothness. The atomic positions are a continuous function of $\mathbf{x}_0^\perp$.

Condition (4): Hard cores. Atoms cannot get closer than a minimum distance r.

As conditions on the atomic surface, we can colloquially paraphrase conditions (2)—(4) to read the surface has no holes or edges; it may be defined locally as a function $\mathbf{x}^\parallel = \phi(\mathbf{x}^\perp)$; there are no branch points or folds on the surface. The strict projection construction corresponds for any D and d to an atomic surface which satisfies all conditions but (3). For the examples in the next two sections we find that the price for smoothing out the surface is a violation of (4).

A family of surfaces satisfying (0)—(4) has a further property that is worth defining formally:

A set of atomic surfaces constitutes an *abstract labeling* if it consists of smooth disjoint connected surfaces, each with a 1:1 projection onto the normal plane, and with a minimum spacing r in the physical direction(s) between any two members of the family.

Clearly, if a family of surfaces constitutes an abstract labeling, then each surface yields one and only one atom (for any $\mathbf{x}_0^\perp$); these atoms will not come closer than the minimum distance r, and they will move continuously under displacements in $\mathbf{x}_0^\perp$. Thus conditions (2)—(4) are obviously satisfied. It is a rather more important point that conditions (2)—(4) can only be satisfied if we have a family of surfaces which constitute an abstract labeling. Thus, conditions (2)—(4) *force* a very simple structure on the way pieces of atomic surfaces (we called them *patches* above) from various D cubes join into larger surfaces.

To see that conditions (2)—(4) imply abstract labeling, note that the atoms move continuously under displacements of $\mathbf{x}_0^\perp$, and thus each traces out a surface as we move the physical plane around. Since the two atoms remain separated, each of them traces out its own surface. Thus we get a set of disjoint surfaces, one for each atom. Continuity then implies the 1:1 property for each of these surfaces.

Enumerating these atomic surfaces labels the atoms. These labels do not permute when $\mathbf{x}_0^\perp$ is taken around in a small closed loop. An abstract labeling can be made concrete if, for example, we can assign d-tuples of integers to each atomic surface in the family, such that no d-tuple is repeated or is missing. In the $3 \rightarrow 1$ example above, this could be accomplished by taking three integers specifying a given cube in three dimensions and adding an integer linear combination of vectors Γ in order to reduce them to a standard form, say, $(0,0,n)$. (Recall from Sec. II that Γ was a set of vectors pointing toward those cubes whose surfaces joined smoothly with a surface inside a given cube.) We call this operation *modding out* by Γ. The resulting integer n would be a label for that atom on a $d = 1$ line which came by projecting the center of the cube whose coordinates were modded out. Note that here the set Γ has exactly $d_\perp$ linearly independent vectors ($d_\perp = 3 - 1 = 2$ in this case). We will see that this is no longer true in the $4 \rightarrow 2$, $5 \rightarrow 2$, and $6 \rightarrow 3$, cases, where the number of independent vectors is D, which is certainly greater than $d_\perp$. We could then try to just keep $d_\perp$ out of D modout vectors. Using them, we would get a unique label for each atom, with gaps in the set of d-tuples describing atoms for a given physical plane. Gaps in the set of labels for atoms is not a problem, but it turns out that this set *depends on* $\mathbf{x}_0^\perp$, i.e., the location of the physical plane, which certainly is a problem.

To see that these consequences of the modding out procedure are not peculiar to it, study a general question of labeling atoms for the projection method. If we could divide all cubes into classes such that when cubes from one class are projected into a normal plane, their images do not overlap and leave no gaps (i.e., they tile a normal plane), then any given physical plane would hit one and only one cube from each class. Labeling these classes of cubes would label atoms, and in such a way that no labels would be lost or acquired as we vary $\mathbf{x}_0^\perp$. (Note that we no longer attempt to label atoms in any special way, like d-tuples of integers of the modout procedure above. This was our motivation for the term "abstract labeling" introduced above.)

In the $3 \rightarrow 1$ and $4 \rightarrow 2$ cases, $d_\perp = 2$. Projection of a 3-cube into a two-dimensional plane is a hexagon; that of a 4-cube is an octagon. Hexagons can tile a normal plane, but octagons will not. In the $5 \rightarrow 2$ and $6 \rightarrow 3$ cases, $d_\perp = 3$, and when projected into three-dimensional (3D) plane, those cubes yield tiles in the shape of rhombic icosahedron and triacontahedron, respectively. None of those shapes will tile a 3D space. We have shown in the previous paragraph that for atoms to be labelable, we ought to be able to find a set of D-cubes, such that their projections tile a normal plane without gaps or overlaps. We conclude that only the $3 \rightarrow 1$ projection will be labelable. One can show that in general the $n \rightarrow (n-1)$ and $n \rightarrow 1$ cases are labelable.

Thus there is no way to label atoms for $4 \rightarrow 2$, $5 \rightarrow 2$, and $6 \rightarrow 3$ *projections* in a way that labels would not appear or disappear as we move $\mathbf{x}_0^\perp$. This is one way to prove a fact—established in subsequent sections by an explicit construction—that no smoothing out of atomic surfaces for those projections would yield an abstract labeling, i.e., a set of 1:1 and onto disjoint surfaces.

While the argument is simple in *projection* cases, we should explore more general situations. Take, for example, a family of surfaces defined by x_1, x_2, x_3 equal an arbitrary triple of integers. Its intersections with the physical plane would be an ordinary crystal; clearly, with no icosahedral symmetry. We could try to enforce the icosahedral symmetry on a family of surfaces by applying 120 elements of the icosahedral group in 6D (see Appendix A for details) to the initial family to generate a set of surfaces. We would get a family defined by $x_{i_1}, x_{i_2}, x_{i_3}$ equal an arbitrary triple of integers for all possible choices of i_1, i_2, and i_3, i.e., it is all 3D planes in a 6D space obtained by piecing together all the 3D faces of all the unit cubes in six-dimensional space. It is obvious that there

are many intersections among different surfaces in this case. Also note that this example has nothing to do with the smoothed out version of the conventional projection method.[31]

The example above is just a particular case of a general theorem we will prove in the remainder of this section that conditions (1)—(4) plus noncrystallographic symmetry imply intersections of surfaces, which is incompatible with condition (4). The result is not confined to projectionlike cases.[32]

To prove this central result, we explore first the consequences of translational symmetry and then add the condition of noncrystallographic symmetry to it.

B. Consequences of translational symmetry

We are generally interested in studying the possibility that patches of atomic surfaces from various cubes connect into a family of surfaces that constitutes an abstract labeling. We show here that if that happens, translational symmetry considerably restricts the resulting class of surfaces. In the process we will uncover some more widely applicable notions. The more general cases will be mentioned after the lemma that follows.

There is only a finite number of patches in each cube, since otherwise atoms would sit on top of each other. Translational symmetry implies that each cube contains identical set of patches. We can now state the following lemma.

Lemma. If the family of atomic surfaces constitutes an abstract labeling, then (a) each surface of the family has a lattice structure, i.e., possesses a discrete translation symmetry group, $T_\perp$. (b) This lattice is a $d_\perp$-dimensional subgroup of Z^D, the lattice of the full D-dimensional space. (c) As a result, every surface in the family remains within a fixed distance of a rational $d_\perp$-dimensional plane.

Remarks. (i) Notice that in general different members of the family may have different lattices. This does not mean that there is complete arbitrariness. In fact, under certain rather general conditions, which are realized in the cases of interest to us, there are severe restrictions on the extent to which $T_\perp$ may differ from one member to another. These are partly explored later in this section. (ii) Notice that (c) of the lemma is much more restrictive than the 1:1 and onto conditions implied by abstract labeling alone. The new restriction is a major consequence of the added condition of translational invariance.

Proof. Each cube contains in general several types of patches. Consider all patches of a given type that lie on one atomic surface. Clearly, one patch of a given type shifts into another patch of the same type under translation by a vector that connects the centers of their respective cubes.

Since we assume the surfaces constitute an abstract labeling, they are infinite in extent. Then each surface contains an infinite number of patches. As there is only a finite number of patch types, there are two patches of the same type within one surface. By translational symmetry, the way the surface looks from the first patch is identical to the way it looks from the second. If the vector that shifts the first patch into the second is then applied to *any* other patch within that surface, even of a different type, we move it into another patch of its own type.

Thus we get one-dimensional "strings" of patches in the surface. Stated another way, we have shown that our surface has a one-dimensional discrete translation invariance. This is not its entire translation group, however. The complete translation group is $d_\perp$-dimensional. Indeed, since the surface projects 1:1 and onto the $d_\perp$-dimensional normal plane, it cannot consist of a finite number of "one-dimensional strings" (unless $d_\perp = 1$). Again, the number of string types is finite since the number of patch types is. Then there is a vector, linearly independent of the previous one, that shifts a whole string into an identical one. Using translational invariance as before, we get that this vector is also part of the translation group of the surface. Continuing this argument, we see that the translation group of the surface is precisely $d_\perp$-dimensional.

A continuous $d_\perp$-dimensional surface with a $d_\perp$-dimensional translation group (lattice) has to stay within a finite distance from the $d_\perp$-dimensional plane spanned by the vectors in that group. Observe also that by construction the vectors in this group are integer-component vectors in a D-dimensional space. Thus the plane that approximates our surface is a *rational* plane in the D-dimensional space. Q.E.D.

Remark 1. The examples in Secs. IV and V generate surfaces which do not satisfy conditions (2)—(4) so that the lemma as stated does not apply. Still, in those sections we will have surfaces obtained from the periodic set of patches within D-cubes. However, the resulting surface(s) will not constitute an abstract labeling. If we go through the proof above, we can see that we may still assert the existence of a translation group within individual connected components of the surface. Its dimensionality may even be greater than $d_\perp$. In the case of surfaces corresponding to the smoothed out $5\rightarrow 2$ or $6\rightarrow 3$ projection method, the lattices are five- and six-dimensional, respectively. That is, the patches from various cubes will be seen to connect into one or several surfaces, each, in fact, penetrating every cubic unit cell of the higher-dimensional space.

Remark 2. If $d_\perp \geq D/2$ as in the $4\rightarrow 2$, $5\rightarrow 2$, and $6\rightarrow 3$ cases, and if we have an abstract labeling, we can make a stronger statement about the surfaces that constitute the labeling than the lemma does. Namely, all the approximating rational planes for different surfaces have to be parallel.

Indeed, if they are not, we can see that due to the conditions on their dimensionality, the two nonparallel approximating planes have to intersect. Since the surfaces they approximate stay within a finite distance from their respective planes, those surfaces also have to intersect, which contradicts our assumption that they are part of an abstract labeling.

Remark 3. Since we have a finite number of patches within each cube, there is a finite number of surface types, all surfaces of one type being obtainable from each other by translation. A group of surfaces of identical type is then labelable by elements of a quotient group $Z^D/T_\perp$,

which is in general a direct product of Z^d and a finite cyclic group. Since there is only a finite number of surface types, the atoms are labelable by a set of d-tuples plus a discrete index with a finite number of values.

Remark 4. In the smoothed out version of the projection method we only have on patch in a cube. If the resulting surfaces were an abstract labeling, there would be only one kind of surface, and we would be able to label atoms by d-tuples of integers without gaps or repetitions. This shows that our definition of "modding out" procedure in Sec. II was not arbitrary. It also means that the simple tiling argument above, which showed the impossibility of enumerating the atoms in a sensible way, does indeed imply that the resulting surface has to be pathological.

Remark 5. The fact that the approximating rational planes are parallel for $d_\perp \geq D/2$ implies a restriction, mentioned before the proof of the lemma, on the variations of $T_\perp$ from surface to surface. When $d_\perp \geq D/2$, the translation group $T_\perp$ of each surface has to be contained in the group of those vectors of the full D-space that are parallel to the set of approximating rational planes.

One may ask whether the lattices of all those surfaces, even those of different types, are not only subgroups of the above-mentioned group, but actually coincide with it. The quotient group $Z^D/T_\perp$ of Remark 3 would then be simply Z^d. We could then label our atoms by d-tuples, without any discrete index.

Unfortunately, it is not true, except in the trivial cases of $d=1$. We have constructed a counterexample, that we do not reproduce here, for other choices of d. One can have a periodic surface, approximated by a rational plane, whose translation group is more "sparse" than the set of vectors of the full D-lattice parallel to this rational plane.

Now that we have a much better idea how the surfaces constituting an abstract labeling look, it is time to see why the abstract labeling is incompatible with noncrystallographic symmetry.

C. Consequences of noncrystallographic symmetry

We have so far only assumed that when we translate all our atomic surfaces in D dimensions by a cubic lattice period, patches from one cube map to patches in another one, and, as a consequence, we have an identical set of patches in each cell. We now study the case when the symmetry group is not merely a translation group, but is a larger (D-dimensional) *space group*— in general containing rotations and reflections—which leaves the set of patches in D-space invariant (see Appendix A).

If our patches join into surfaces, then each surface goes into another one (or itself) under the action by the elements of this space group. The only space groups that are of interest to us are those that leave the direction of the physical plane invariant. Otherwise, the diffraction pattern and other physical properties of the real d-dimensional space would not be invariant.

We thus add a new condition to conditions (1)—(4) above.

Condition (5): Symmetry. The family of surfaces is invariant under the elements of a D-dimensional space group. The elements of this group also preserve the orientations of the physical plane.

We will discover in this section that conditions (1)—(4) are incompatible with condition (5) for many groups of interest to us: namely, groups with a *noncrystallographic* symmetry. This means they include rotations which are not allowed in any d-dimensional lattice. In particular, fivefold rotation axes are noncrystallographic in $d=3$ and so conditions (1)—(4) are incompatible with icosahedral symmetry. Before making more general statements, let us work out this case.

We have seen that the directions of the physical and normal planes should be preserved by the space group. We know[22] that the only two three-dimensional planes, whose directions are preserved by the six-dimensional space group with icosahedral point group, have irrational orientations.

Now, if our ($d_\perp=3$)-dimensional surfaces constitute an abstract labeling, i.e., satisfy conditions (1)—(4), we know from the previous section that each of them has a discrete lattice, $T_\perp$, associated with it. As a result, each atomic surface stays within a finite distance of a *rational* plane spanned by this lattice. When we apply a space-group-symmetry operation, each surface goes into another one (possibly itself); the approximating plane of the first surface goes to that of the second. But, as we showed in the previous section, all the approximating planes have the same orientation. This means that the corresponding rational subspace must be invariant under the rotational part of the space group (which is known as the *point group).* But our point group leaves only *irrational* 3D planes invariant.

We have thus proven Theorem 1.

Theorem 1. Conditions (1)—(4) are incompatible with icosahedral symmetry.

More generally, if we have an abstract labeling and any space group, then the point group of that space group must leave invariant the rational subspace which approximates the atomic surfaces. The intersection of this subspace and the D-dimensional lattice, is a $d_\perp$-dimensional sublattice. Since the point-group operations map lattice vectors to lattice vectors and leave the subspace invariant, they must in fact leave the sublattice invariant. Furthermore, one can form a quotient of Z^D by the sublattice and this will be a d-dimensional lattice which is also invariant under point-group operations.

Theorem 1 then generalizes to Theorem 2.

Theorem 2. A noncrystallographic D-dimensional space group is incompatible with the physical conditions (1)—(4) of Sec. III A.

This follows from the preceding argument, which showed that conditions (1)—(4) imply the space group operations preserve a d-dimensional[33] sublattice, which contradicts the definition of noncrystallographic. This is a major result of this paper whose implications are further explored in the Discussion.

IV. 4→2 PROJECTION

In this section we will explore the simplest example in which the stepped surface defined by projection cannot be smoothed into a family of surfaces with the properties required for an abstract labeling. The symmetry condition (5) will play no role in this section. We first discuss, in complete analogy to the 3→1 case, how to deform the patch of the stepped surface associated with each cube to eliminate the discontinuities. The algorithm immediately generalizes to higher dimensions. We will continue to refer to this family of surfaces, which are actually all connected through branch points, as "atomic" surfaces even though they do not satisfy all the conditions (1)—(4). In fact, the contents of this section will spell out and hopefully make intuitively obvious why all projections with both d and $d_\perp$ greater than 1 do not give rise to physically reasonable families of atomic surfaces.

In the first subsection we see that the smoothed atomic surface, as defined, is branched, necessarily allowing atoms to get arbitrarily close whenever the physical plane has irrational slope. Merely cutting out the branch points is no solution, since atoms would then appear or disappear when the physical plane passed through the voids. In the next subsection we show that the branch points resemble the Riemann surface for the cubic root in that merely moving the intercept of the physical plane, $\mathbf{x}_0^\perp$, around a small loop results in a nontrivial permutation of three atoms.[34] Three consecutive loops yield the identity permutation. Under the projection method, atoms in the vicinity of these vertices behave in precisely the same way.

The third pathology of our smoothed atomic surface, which is intimately related to the first two, is discussed in the last subsection. Namely, there is really only one connected surface. One can move onto different sheets at the branch points and flow continuously from one cube to any other. As a corollary we show that any atom can be moved by successive permutations into any other atomic site by passing $\mathbf{x}_0^\perp$ around a closed loop in the perpendicular plane. This is the most direct means we have for demonstrating that there is no invariant labeling induced by the smoothed surfaces resulting from the projection method.

A. Definition of atomic surface and branching at vertices

Many of our constructions here are similar to those of the 3→1 case. We define a normal plane whose dimension is $d_\perp = D - d = 2$. The physical planes are labeled by $\mathbf{x}_0^\perp$. We now consider projecting a 4-cube onto the normal plane by dropping a physical 2-plane from each of its points. The resulting figure will clearly be a polygon whose edges correspond to certain 1-edges of the 4-cube. Observe that if both the normal and the physical 2-planes pass through a common vertex of the 4-cube, only one will enter the cube itself. Since the meaning of "normal" and "physical" can be interchanged, there are eight of the sixteen 4-cube vertices with the property that a physical plane passing through that vertex does not enter the cube. Therefore, the cube's projection is an octagon (exceptional orientations of the physical plane are ignored henceforth), with opposite sides parallel.[30] The edges of the 4-cube that project onto the perimeter of the octagon will be termed *silhouetting*, just as we did in Sec. II for the 3→1 case.

Clearly, any point $\mathbf{x}_0^\perp$ within the octagon defines a physical plane which enters the corresponding 4-cube. If one adopts the rule of projecting onto the physical plane the center of every 4-cube it enters, then one implicitly defines a surface which consists of the same octagonal piece of the normal plane through the center of each cube, with steps, as in the 3→1 discussion, which lie above the projection of the silhouetting edges. How the patches of atomic surfaces from various cubes are to be connected is again fixed by demanding continuity in the projection. A given 1-edge is silhouetting with respect to precisely two of the eight cubes which share it. It is the patches in these two cubes which get connected. We show how to smooth out this stepped surface, and then return to the projection construction when we examine the permutation of atoms induced by displacements of the physical plane about a 4-vertex.

To construct the smoothed atomic surface within a single cube, identify those 1-edges of the 4-cube that yield the perimeter of the octagon. They clearly link the vertices that define the octagon and therefore form a closed connected set of silhouetting 1-edges on the cube. Draw one-dimensional segments that connect the cube center to each point on these 1-edges. The result is a smooth two-dimensional surface *patch* that projects 1:1 onto the octagon. More pictorially put, we have lifted the projection back into the 4-cube and suspended it on a closed ring of 1-edges.

These patches of the atomic surface now smoothly extend from cube to cube, eliminating the steps inherent in the projection method yet preserving the topology. The surface patch associated with each cube is now strictly contained in the cube and terminates on the silhouetting edges. Patches from two different cubes join precisely along the silhouetting edges. Since the atomic surface is periodic, we will occasionally use the adjective "extended" to emphasize its repetition through the lattice in analogy with the extended zone scheme in the theory of band structure. It is apparent that the atomic positions that are defined by projection onto the physical plane are in 1:1 correspondence with those defined by this new atomic surface. Since both descriptions are periodic, there is an obvious upper bound on the displacements of atoms required to bring the two atomic patterns into coincidence.

This extended atomic surface has branch points at each 4-vertex, to whose consideration we now turn. Project the eight 1-edges emanating from a given vertex onto a normal plane. The vicinity of the projection of that vertex is then broken up into eight sectors (Fig. 4). Various 4-cubes share these edges and each contains a piece of atomic surface which projects onto an octagon.

Using continuity to work away from the case when the physical plane is oriented in such a way that each octagon is symmetrical, one observes that each octagon spans three sectors (Fig. 4). While $\mathbf{x}_0^\perp$ is inside a particular octagon, the physical plane stays within the corresponding cube and intersects a patch of atomic surface within that cube.

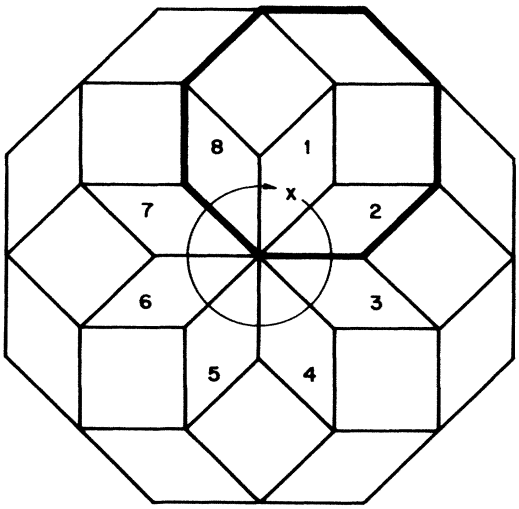

FIG. 4. Projection of the eight unstable cubes at a vertex onto octagons in the normal plane for the 4→2 case. The physical plane projects to a point in one of eight sectors and intersects three octagons; hence three cubes. Under one circuit from sector 1, the octagons (1-2-3),(7-8-1),(8-1-2) (labeled by three sectors each of them covers) permute into (7-8-1),(8-1-2),(1-2-3), respectively.

It only leaves a particular cube when it leaves its corresponding octagon. Suppose we initially have $\mathbf{x}_0^\perp$ in sector 1, as in Fig. 4. Sector 1 in Fig. 4 is covered by octagons (7-8-1), (8-1-2), and (1-2-3), (denoted by three sectors each of them covers). Therefore the physical plane intersects patches of atomic surface inside the three corresponding cubes. Let us see what happens to the point of intersection inside the cube corresponding to octagon (1-2-3) as we move the physical plane in a way prescribed by the loop in Fig. 4. We leave octagon (1-2-3) only when we cross the boundary between sectors 3 and 4, upon which we enter octagon (4-5-6). As we continue, we enter octagon (7-8-1), which we do not leave as we stop in sector 1. Thus making one loop in $\mathbf{x}_0^\perp$ continuously moves a point of intersection with the physical plane (i.e., an atom) from one cube into one in another cube. Three complete cycles moving through all eight octagons are required to make a closed loop in the extended atomic surface. Contrast this picture with the 3→1 projection where a closed loop in the atomic surface projected 1:1 onto the normal plane.

Recall that to actually make the atomic surfaces in the 3→1 case disjoint, it was necessary to pull them apart at certain vertices where three edges from each of the two surfaces met. In higher dimensions, such as 4→2, these intersections cannot be removed. As we have just seen, the branch structure permits one to pass from sheet to sheet without even hitting a singular vertex.

B. Permutations near a vertex

To make contact with the projection construction, recall that the physical plane passing through a vertex enters the interior of eight 4-cubes, henceforth called *stable* and misses eight others, the *unstable* ones. Under small displacements of the physical plane, it will still enter the eight stable cubes and in addition enter three of the unstable ones. This latter observation is made plain by considering the dual grid.[4,5,35,36]

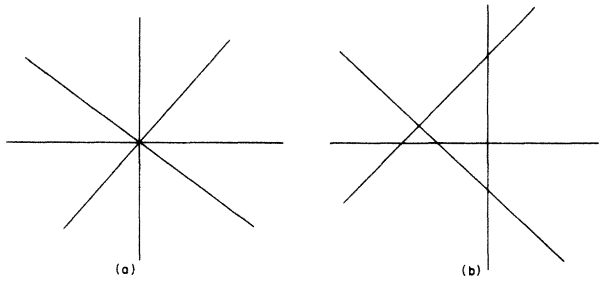

FIG. 5. The dual grid showing the intersection of the coordinate 3-planes with the physical 2-plane, for the 4→2 projection. Each open region corresponds to a definite cube that will get projected onto the plane. Crossing a line changes the corresponding index of the cube by ±1. In (a) the physical plane hits a vertex of the 4-lattice. For generic displacements, the lines appear as in (b). There are eight stable cubes represented by the open sectors and three unstable ones corresponding to the bounded regions.

Intersect the physical plane (defined by $\mathbf{x}^\perp = \mathbf{x}_0^\perp$) with each of the coordinate 3-planes obeying x_i = integer to form four families of equally spaced parallel lines. Each open region defined by these lines represents a 4-cube that the physical plane enters and hence represents one atom in the quasicrystal. When the physical plane is displaced along one of the coordinate axes, only one family of parallel lines moves in the physical plane. Thus we can have arbitrary relative translations of these families of lines as a result of moving the physical plane.

Now, when the physical plane hits a vertex, four lines intersect in a point (Fig. 5). Under small but arbitrary displacements, the diagram generically breaks into three bounded regions and eight open sectors. The latter correspond to the stable cubes since they persist under rearrangements of the lines, while the former correspond to three of the eight possible unstable cubes. Which three depends on the arrangement of lines. All this merely restates Fig. 4 since the octagons there are just projections of the unstable cubes. Relative coordinates of any cubes represented in the dual grid picture can be calculated by adding ±1 to the appropriate coordinate where the line is crossed.

The permutations induced among the three atoms that come from the unstable cubes are most conveniently visualized in our earlier picture of the eight overlapping octagons arrayed around a common vertex. (The central vertex lies in the interior of the octagons for the stable cubes. For small excursions of the physical plane, $\mathbf{x}_0^\perp$ remains in their interior, and it is therefore unnecessary to draw them.) A given sector is covered by precisely three octagons which by definition are the images of those 4-cubes the physical plane with intercept $\mathbf{x}_0^\perp$ enters. Moving $\mathbf{x}_0^\perp$ around a small closed loop on the normal plane induces a cyclic permutation on the three octagons that cover the base point of the loop.[34]

C. Nonexistence of invariant labeling

The last property to establish is that the extended atom-

ic surface drawn from one 4-cube enters a finite fraction of all the 4-cubes on the lattice. Call γ_i the difference between the centers of the two adjacent cubes whose surfaces join smoothly through a silhouetting 1-edge. There are precisely eight silhouetting edges in a cube, which correspond to the eight sides of the octagon. They result in eight γ_i, and those come in plus-minus pairs. The components of the 4-vectors γ_i are clearly ± 1 or 0. It suffices to show that one can choose four γ_i such that their determinant is nonzero, since then their integer combinations will span a finite fraction of the lattice. Note that in the $3\rightarrow 1$ case we had only two, and not three linearly independent γ_i.

To prove the above assertion about the determinant, note that we could have defined γ_i as the vectors connecting the midpoints of the opposite silhouetting edges in the cube. Under projection γ_i have to become vectors connecting the midpoints of the opposite sides of the octagon. To find out what the components of the γ_i were in the four-dimensional space, note that the sides of the octagon coincide with the projections of the four unit vectors. Assign a particular direction to each of the four pairs of sides in the octagon, which gives us four vectors. We easily find which integer linear combinations of these four vectors give the vectors connecting the midpoints of the pairs of opposite sides in the octagon. It turns out that the determinant is equal to 1.

As a corollary, note that any two atoms on the physical plane correspond to 4-cubes related by an integer combination of γ_i. Then there exists a *closed* loop in the normal plane such that the first atom is permuted into the location of the second. The demonstration is immediate. Since the two cubes are related by an integer combination of γ_i, and individual γ_i just show which two cubes have their surfaces connected, we can find a sequence of cubes whose surfaces join in one connected surface that links those inside the two cubes in question. Connect the two atoms by a path of this extended atomic surface and project onto the normal plane. The initial and final points in the normal plane are identical since the two atoms are on the same physical plane. When $\mathbf{x}_0^{\perp}$ moves around the indicated loop on the normal plane, the desired permutation occurs.

The existence of nontrivial permutations when $\mathbf{x}_0^{\perp}$ traverses a closed path precludes the existence of an abstract labeling as previously defined. Clearly, the smooth atomic surface also violates condition (4). We also see more clearly the content of the tiling argument on the normal plane in Sec. III. Too large a D generates a zonogon[30] "tile" which is too complicated to tile $d_{\perp}$-space, so that there are more than $d_{\perp}$ independent γ_i.

V. THE $5\rightarrow 2$ AND $6\rightarrow 3$ PROJECTIONS

The $5\rightarrow 2$ and $6\rightarrow 3$ projections are physically interesting since for special choices of the orientation of the physical plane they yield the "decagonal" and icosahedral symmetries observed experimentally.[1,2] At several stages we will be more quantitative than in the previous section and use these special directions. In the $5\rightarrow 2$ case we follow de Bruijn[5] and define the physical plane by

$$\mathbf{x}^{\parallel}=r_1\mathbf{t}_1+r_2\mathbf{t}_2\ ,$$
$$(t_1^i,t_2^i)=(\cos[2\pi(i-1)/5],\sin[2\pi(i-1)/5])\ . \tag{1}$$

Since our primary interest is to explore the topological properties of atomic surfaces in the simplest setting possible, we first deviate from de Bruijn in allowing the physical plane to sit anywhere within the 5-cube rather than imposing the one linear constraint that leads to Penrose's tiling. At the end of this section we outline changes necessary to treat the Penrose case, which is of primary interest for the decagonal phase.[2] The presentation is more formal than in the previous section, since otherwise the results, which are simple to state, would get lost in the demonstrations. The two cases are initially considered in parallel.

A. Atomic surfaces and their extension

We will follow our earlier procedure of projecting the D-cube ($D=5,6$) onto the normal $d_{\perp}$-plane ($d_{\perp}=5-2=6-3=3$) and lifting the resulting figure back into the D-cube. The atomic surface so defined will again be a smoothed version of the stepped surface which is equivalent to the projection of the cube center.

We first describe an explicit algorithm for computing which two-dimensional faces of the 5-cube will form the boundary of the 5-cube's projection into a normal plane.

The 5-cube projects to a convex three-dimensional body, whose faces correspond to certain 2-faces of the 5-cube. By analogy with the $3\rightarrow 1$ and the $4\rightarrow 2$ cases, we call them *silhouetting* 2-faces.

Observe that a 2-face will become a part of the boundary of the 5-cube projection into a normal plane if and only if the projecting physical plane will *not* enter the interior of the 5-cube when it is drawn through a point on that 2-face. Otherwise that point has to project into the interior of the 5-cube's image. We next give an algorithm for identifying all the 2-faces of a cube such that a physical plane drawn through any point on one of these 2-faces will not enter the cube.

The normal plane is defined by three vectors that span it, $\mathbf{n}_i$, $i=1,2,3$. Pick any two of the five coordinates, say 1,2. Then there is a unique line in the normal space whose five-dimensional tangent 1 satisfies $l_1=l_2=0$. Let $\sigma_i=\mathrm{sgn}(l_i)$. There are $\binom{5}{2}=10$ choices of the two coordinates that we can make zero in this way. We then get ten vectors which have two coordinates equal to zero and three coordinates equal to ± 1. If drawn from a 5-cube center, these vectors and their inverses will point toward twenty 2-faces (out of 80) of the 5-cube. Our claim is that these are precisely the silhouetting 2-faces.

To see why a physical plane drawn through a 2-face defined, say, by the vector $\gamma=(0,0,\sigma_3,\sigma_4,\sigma_5)$, does not enter the cube, observe that to enter the cube through such a face the physical plane has to contain a line with a tangent vector whose signs are $(\pm,\pm,\sigma_3,\sigma_4,\sigma_5)$, where the first two entries are arbitrary. Notice, however, that $(0,0,\sigma_3,\sigma_4,\sigma_5)$ were chosen to be the signs of a vector in the normal plane, and $(\pm,\pm,\sigma_3,\sigma_4,\sigma_5)$ to be the signs of the vector in the physical plane. It is easy to see that the scalar product of two such vectors is positive, so they can-

not be perpendicular. Thus the physical plane cannot enter the cube through such a 2-face, and we have verified our assertion.

In the 6→3 case we still look for 2-faces as the dimension of the normal space is still $d_\perp = 3$. We can select two of the six components in $\binom{6}{2} = 15$ ways, and thus the above procedure yields $15 \times 2 = 30$ silhouetting 2-faces.

We have therefore:

Lemma 1. The unit 5 (6) -cube projects onto a 20 (30) -faced solid, a polyhedron with 22 (32) vertices.

The assertion about the number of vertices will become more obvious later. It is just the number of vertices of the 5 (6)-cube such that the physical plane drawn through such a vertex does not enter the cube. As for the 2-faces above, only these faces of the hypercube will project onto the boundary of its image in the normal plane.

The proof above is rather technical, but is easily converted into a computationally convenient algorithm for enumerating the silhouetting 2-faces. Vectors[37] that define the silhouetting 2-faces for the 5→2 and the 6→3 cases are given in Table I.

For the special decagonal (icosahedral) symmetries the polyhedron becomes a rhombic icosahedron (triacontahedron). A sketch of the latter object is found, say, in Refs. 20, 24, and 26, whereas a picture of the former appears below (Fig. 9).

One could use a more geometric approach to calculating the vectors of Table I. These vectors are the same as those connecting the centers of opposite silhouetting 2-faces in the D-cube. Upon projection into 3D space, they become vectors connecting the centers of the opposite faces on the cube's image (zonohedron[30]). The edges of this polyhedron are just projections of the unit vectors of the D-space. Just like we did for the octagon in the 4→2 case (see Sec. IV), we can find which integer linear combinations of the sides give the vectors connecting the 2-faces.

We now start constructing the smoothed out atomic surface,

Construction. The patch of the atomic surface is the union of all line segments which connect the cube center with all points on the silhouetting 2-faces.

As before we can show the patch is smooth and has a 1:1 projection into the normal plane. Just as in the 3→1 and 4→2 cases above, this patch is part of a smoothed out version of the stepped surface needed to define the projection method. As before, it is as though we took the (now three-dimensional) "shadow" of the cube in the normal plane and suspended it on the silhouetting 2-faces of that cube.

We next consider how the atomic surface extends beyond a single cube. Our patches by construction terminate only on the silhouetting 2-faces. Thus the patches in the two adjacent cubes can be connected smoothly only across a common silhouetting 2-face. It is crucial that there is only one other cube for which that 2-face is also silhouetting. Then given a silhouetting 2-face in a cube, we unambiguously extend a surface through that 2-face into one of the adjacent cubes.

To prove this fact, recall that we enumerated silhouetting 2-faces above by vectors γ_i which pointed toward the centers of those faces from the center of the cube (Table I). Properly normalized (by a factor of $\frac{1}{2}$), those vectors would terminate exactly at the centers of those 2-faces. If the 2-face is silhouetting with respect to two cubes that share it, there are two vectors in Table I, say, γ_1 and γ_2, such that $\frac{1}{2}\gamma_1$ and $\frac{1}{2}\gamma_2$ extend from the centers of the two cubes toward the center of that 2-face. Then $\frac{1}{2}(\gamma_1 - \gamma_2)$ is a vector connecting the two cube centers. Since all our γ_i have two entries zero, the rest being ± 1 (Table I), if γ_1 is not parallel to γ_2, we are going to get $\frac{1}{2}$ as one of the en-

TABLE I. The first half of the table shows the vectors which, together with their inverses, point toward the 20 silhouetting 2-faces in the 5→2 case. The second half shows vectors defining 30 silhouetting 2-faces of the 6→3 case. Vectors 1, 2, 7, 8, and 10 of the 5→2 column give a determinant equal to 1; this is one of many possible choices. Vectors 1, 2, 3, 4, 6, and 7 of the 6→3 case give a determinant equal to 2. In both cases these are the lowest nonzero values of determinants.

	Vectors for 5→2						Vectors for 6→3						
1	0	0	1	−1	1	1	0	0	1	−1	1	−1
2	0	1	0	1	1	2	0	1	0	−1	1	−1
3	0	1	1	0	1	3	0	1	−1	0	1	−1
4	0	1	−1	1	0	4	0	1	−1	1	0	−1
5	1	0	0	1	−1	5	0	−1	1	−1	1	0
6	1	0	1	0	1	6	1	0	0	−1	1	−1
7	1	0	1	1	0	7	−1	0	1	0	1	1
8	−1	1	0	0	1	8	−1	0	1	1	0	1
9	1	1	0	1	0	9	1	0	−1	1	−1	0
10	1	−1	1	0	0	10	1	−1	0	0	−1	1
						11	−1	1	0	1	0	1
						12	−1	1	0	1	1	0
						13	1	1	−1	0	0	−1
						14	−1	1	1	0	1	0
						15	1	−1	1	−1	0	0

tries in the vector above, which is impossible if it connects two cube centers. Thus, γ_1 and γ_2 are parallel and shift one of the two cubes into another.

We thus not only verify the assertion above, but also get a practical calculational rule that patches in the two adjacent cubes join smoothly whenever the two cubes are related by a shift with a vector from Table I.

We have established the first part of Lemma 2.

Lemma 2. The 10 (16) difference vectors between opposite silhouetting 2-faces give all the shifts which extend the atomic surface. The extended atomic surface from a given D-cube enters every cube for $D=5$ and every other cube for $D=6$.

The second statement in Lemma 2 follows in the $5\rightarrow 2$ case by showing that there are 5 vectors in Table I whose determinant is ± 1. They therefore constitute a set of basis vectors for the lattice equivalent to the original ones. For the $6\rightarrow 3$ case the analogous calculation yields a determinant of ± 2. It is simple to show for any orientation of the physical plane that the determinant, if nonzero, is no less than 2. Define the parity of a cube to be the parity of the product of its six-integer labels. When one passes through a 2-face, the parity is unchanged for $D=6$ implying that the even and odd cubes do not mix.

We can repeat the argument at the end of Sec. IV and emply Lemma 2 to prove, for the $5\rightarrow 2$ case, Theorem 1.

Theorem 1. Given any two atomic positions on the physical plane, there exists a closed loop in the normal plane such that when the physical plane is moved around it, the atom in the first position moves to the second location.

This also holds for the $6\rightarrow 3$ case with the only difference that we only connect two atoms that come from the cubes of the same parity.

One may conjecture that all (even) permutations of an infinite quasicrystal are generated by loops in $\mathbf{x}^{\perp}$. This is much stronger than Theorem 1 above, where we do not control what other atoms do when the one in question is moved.

B. Atomic surface structure near a vertex

Following our earlier discussion, we first enumerate the cubes the physical plane enters in the vicinity of a vertex. We then project some of the D-cubes that share a given vertex onto the normal plane and examine how they permute under small displacements of the physical plane. The permutations are identical whether we place the atoms by strict projection or intersection with the smoothed atomic surface.

We define a *stable* cube at a vertex to be one which the physical plane always enters if it is close enough to the vertex. The permutations will act on the remaining unstable cubes. To determine the number of unstable cubes the physical plane enters at a time, we again construct the dual grid.

For $5\rightarrow 2$, intersect the physical 2-plane with the five families of 4-planes, $x_i=$integer, to generate five sets of parallel lines. When the physical plane hits a vertex, five lines meet in a point forming ten sectors. When the physical plane is displaced, six more regions are formed (Fig. 6). Each region in the figure corresponds to a definite cube since each index changes by ± 1 when we cross the corresponding line. The ten unbounded sectors correspond to the stable cubes. Thus there are $32-10=22$ *unstable* cubes at the vertex. The six bounded regions in the figure show that the physical plane generally enters six out of the total of 22 unstable cubes at the vertex.

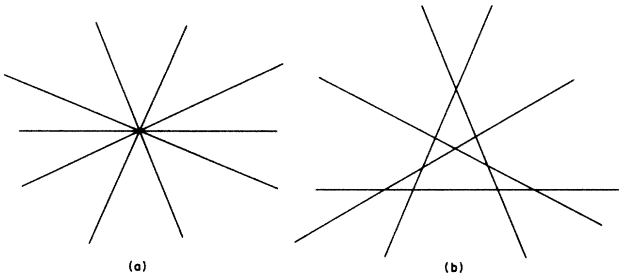

FIG. 6. The dual grid for the $5\rightarrow 2$ case; showing in (a) the intersection of the coordinate 4-planes with the physical plane through a vertex. In (b) the physical plane was displaced to generate the six unstable and ten stable cubes.

For $6\rightarrow 3$, we need a formula from Appendix B for the number of regions six 2-planes divide the physical 3-plane into. We therefore have Lemma 3.

Lemma 3. In the vicinity of a vertex for the $5\rightarrow 2$ ($6\rightarrow 3$) projection, the physical plane enters 10 (32) stable cubes and generally 6 (10) unstable ones drawn from the remaining 22 (32). The number of possible unstable cubes equals the number of vertices of the rhombic icosahedron (triacontahedron).

The latter statement follows from the following considerations. Draw the physical plane through a vertex of a cube. If the plane does *not* enter that cube, then this vertex must be on the boundary of the cube's image in the normal plane. The number of vertices for which the plane will enter the cube can be found by considering 2^D cubes sharing a common vertex. If we draw a physical plane through the vertex, the number of cubes it enters is the same as the number of vertices in a single cube through which the plane does enter.

1. $5\rightarrow 2$ case

For the $5\rightarrow 2$ case it is simple and informative to visualize the tilings that are generated near a vertex. That is, we want the dual to the dual grid we employed above, or just the projection of the cube centers onto the physical plane. The ten stable cubes form the perimeter of a decagon with six additional vertices in the interior which permute about (Fig. 7). In the dual picture, the elementary rearrangement is one line passing through the intersection of two others (Fig. 8). Provided that the excursion of $\mathbf{x}_0^{\perp}$ in the normal direction is sufficiently small, the outer boundary of the decagon is left unchanged. Each step of

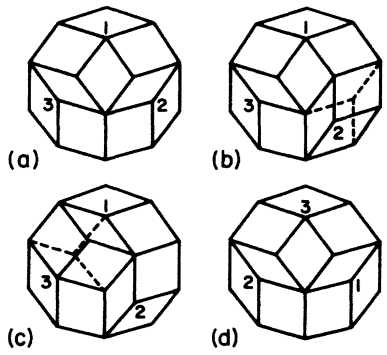

FIG. 7. Permutations of vertices within a decagon of the two-dimensional Penrose tiling. (a),(b),(c) Show two-step transformations of decagon through jumps (old configuration indicated by dashed lines). (d) Result of ten iterations of the two-step transformation. The vertices (labeled 1,2,3) have permuted. The other three interior vertices also permute cyclically.

the transformation is a repacking of a hexagon with a jump of one vertex within it (recall Fig. 8). All possible decagons (see Fig. 11 below) can be reached by such jumps: each sequential pair in Fig. 11 is related by one jump.

Now, in Fig. 7 we can go from (a) to (b) to (c) by single jumps. But Fig. 7(c) is the same type as (a), except it is rotated by an angle of 108°; also, in (c) atom 1 is in the place corresponding to atom 2 in (a), etc. If we repeat this two-step process ten times, we will return to the original orientation but the atoms will have permuted cyclically, as in (d).

The permutations induced among the unstable cubes by displacements of the physical plane could thus be enumerated by a close examination of the possible tilings of a decagon.[38] We prefer, however, to project all the unstable cubes at a vertex onto the normal 3-plane, count the number of three-dimensional sectors into which they divide the space, and finally display the generators of the permutations by examining how selected atoms permute as $x_0^{\perp}$ moves through the sectors. Just to display the sectors, the projection may be reduced to considering the intersection of the surface of a sphere about the vertex with the image of the D-cube. In the $4\rightarrow 2$ case, this would correspond to marking off eight sectors on a *circle* and associating each successive group of three with an octagon. We first work the $5\rightarrow 2$ case to completion.

The 20 faces of the rhombic icosahedron (RI) define ten 2-planes in the normal 3-plane. The 22 unstable 5-cubes project into the 3-plane as 22 RI sharing a vertex. Their faces at that vertex piece together to become ten great circles when intersected with a small sphere around the common vertex. All ten circles are necessary to represent the 22 unstable cubes. As before, the central vertex projects into the interior of the RI for all the stable cubes, which are not involved in the permutations. From the formula in Appendix B, there are at most $2[\binom{9}{0}+\binom{9}{1}+\binom{9}{2}]=92$ regions cut out by these circles and hence at most 92 out of $\binom{22}{6}$ sets of six 5-cubes represented on any physical plane. The actual number is somewhat less since symmetries force more than two great circles to meet in a point.

Looking at the RI, one can identify five groups of eight faces each, which are just closed bands of rhombi attached side by side (Fig. 9). Each face is included in the two separate bands defined by its edges. When we collect together the 22 RI, which share a vertex, the faces from different RI, but in a common group, will piece together into four planes, all containing a common line. The line becomes two points on the surface of the sphere, and we lose a total of $2\times 3=6$ regions (Fig. 10). There are five such groups of faces for a loss of 30 regions. By direct enumeration we see there are only $92-30=62$ distinct tilings of a decagon (Fig. 11). Therefore, we have shown for the $5\rightarrow 2$ case, Lemma 4.

Lemma 4. There are 62 different arrangements of 6 out of 22 unstable cubes at a vertex each of which corresponds to a tiling of a decagon by rhombi. All possible tilings of a decagon may be obtained by projection.

Note that it was not necessary to use the pentagonal symmetry to prove Lemma 4. An affine transformation changes directions, yet leaves parallel lines parallel, which is all that is actually needed to prove Lemma 4. The grouping of faces we exploited, follows from the fact that there are only five directions a 1-edge in the 5-cube can point in. Parallel edges remain parallel under any projec-

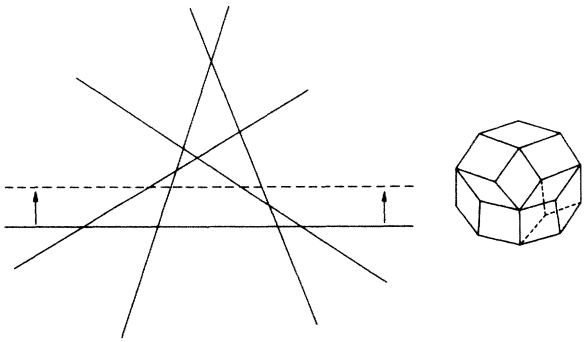

FIG. 8. The dual grid and its associated tiling obtained by projecting the 5-cubes that the physical 2-plane enters near a vertex. The dashed tiles show the effect of moving one line through the intersection of the two others in the dual picture.

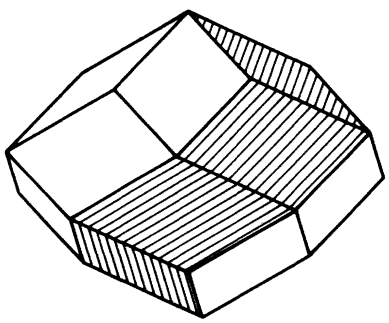

FIG. 9. A rhombic icosahedron with 20 faces and 22 vertices. There are eight bands which tie together the parallel edges. One of them is shown here.

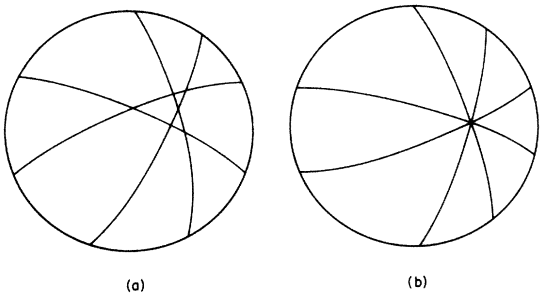

FIG. 10. Each group of eight faces on a rhombic icosahedron falls onto four planes passing through a common line when the 22 unstable 5-cubes are projected onto the normal 3-plane. Three regions disappear from the generic picture on the left.

tion. The common edges in the five bands of rhombi above are five such classes of parallel edges.

To enumerate the permutations, we have to mark off what we call *spherical polygons* formed by the intersections of single RI with the sphere's surface. They are convex and can have 3, 4, or 5 sides each of which is an arc of a great circle. Any point on the sphere's surface will be in six spherical polygons. Now draw a loop on the sphere, record the six RI covering the base of the loop, and follow along the curve until reaching the boundary of the RI in question. Record the new RI and continue along the loop until it closes and the RI finally returns to one of the six present at the base point. There is a complete analogy to the $4\rightarrow 2$ case except that there are several centers which induce nontrivial permutations.

All vertices of the spherical polygons occur at the points where four great circles meet. This is because all rays from the center to a vertex are parallel to the edges from one of the groups of faces mentioned above. Loops that encircle the intersections of two great circles do not generate any permutations of the cubes. By explicit calculation, each fourfold point, when encircled, induces a 3-cycle permutation on three of the six cubes which exist in any one of the regions on the sphere. Each of the 10 fourfold points will induce the same cycle on 3 out of 22 possible unstable cubes. To construct the entire group, we connect a fixed base point to the vicinity of each of the 10 fourfold points, perform the permutation, and then loop back to the base. In this way all even permutations in S_6 (permutations of 6 objects) are generated.

Theorem 2. Any even permutation of the six untable cubes at a vertex in the $5\rightarrow 2$ problem can be generated by moving the physical plane around a small closed loop in the normal plane.

The details of the calculation may be found in Appendix C.

2. $6\rightarrow 3$ case

This projection proceeds analogously to the previous case except that there is more degeneracy when the triacontahedra intersect the sphere. The triacontahedron has 30 faces, opposite ones parallel, which reassemble to 15 great circles when we project the 32 unstable 6-cubes that share a vertex. The total number of possible regions on the sphere is $2[\binom{14}{0}+\binom{14}{1}+\binom{14}{2}]=212$. In the case of icosahedral symmetry, the triacontahedron has six fivefold axes, with a band of ten faces about each, where each band results in a total of five different great circles intersecting at one point, which occurs twice at the two opposite points on the sphere, resulting in a loss of $2\times 6=12$ regions (Fig. 12). The six bands thus eliminate $6\times 12=72$ regions from the 212 present for generic planes. There are also ten threefold axis which each eliminate one region for each of the two antipodal points in which they intersect the sphere, thus further reducing the number of regions by 20. With all these symmetries, there remain $212-72-20=120$ distinct regions on the sphere, each corresponding to a distinct tiling of a triacontahedron with rhombohedra. The 32 stable cubes correspond to the vertices of the triacontahedron. The ten unstable ones become the vertices of the rhombohedral tiles that fall inside the triacontahedron.[39] These tilings produce a representation of the 120 element icosahedral group. None of the tilings have any symmetry, and the group generates them

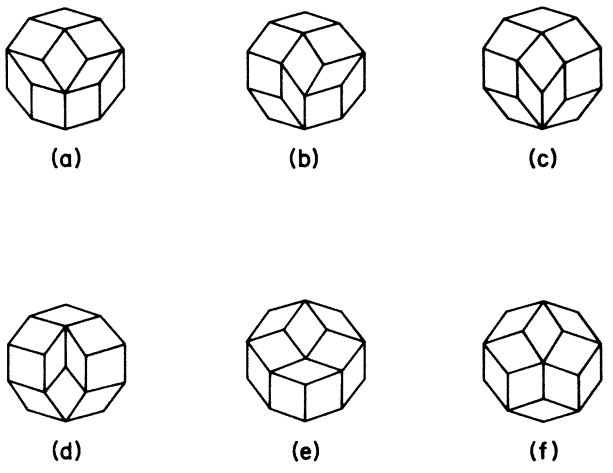

FIG. 11. All tilings of a decagon up to symmetry. Diagram (b) has no particular symmetry and generates 20 tilings under rotations and reflections. Diagrams (a), (c)—(e) have an axis of symmetry and generate 10 tilings each. Figure (b) has a fivefold axis, so it contributes only 2 more for a total of 62.

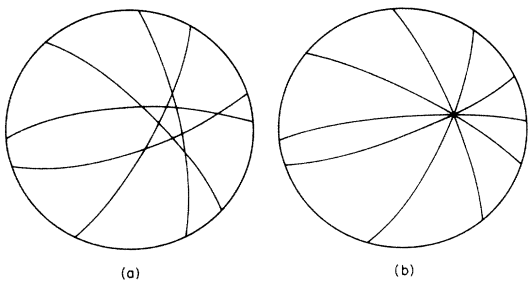

FIG. 12. Five great circles, formed from the faces of the 32 projected unstable cubes have a point in common. Six regions are eliminated from the sphere in each hemisphere, and it happens for each of the six fivefold axes.

all from any one.[40]

We have therefore shown Lemma 5.

Lemma 5. There are 120 distinct arrangements, each involving 10 out of the 32 unstable cubes at a vertex, that generate different tilings under projection.

The permutation group on the ten inner vertices can again be constructed by tracing the spherical polygons that a closed loop moves through on a sphere. Only the six points where five circles intersect are of interest since the vertices of the spherical polygons can only fall there. By explicit computation we establish Theorem 3.

Theorem 3. Of the ten unstable 6-cubes represented on any one physical plane, three have odd parity and seven have even parity. Moving the physical plane in a small loop around the vertex generates all even permutations of the even and odd unstable cubes at that vertex. This group of permutations is just all even permutations of $S_3 \otimes S_7$.

C. The case of constrained and "proper" Penrose tilings

In the case of the two-dimensional Penrose tiling with fivefold symmetry, the physical plane is actually commensurate in one dimension since one of the vectors normal to it is $\mathbf{t}_5=(1,1,1,1,1)$. Consequently, in this case one would not expect a shift in the $\mathbf{t}_5$ direction to be a symmetry of the system; in the projection construction, for instance, one finds tiling with different kinds of local order which would have different total energies under a generic Hamiltonian.[10,24,27,28,41,42]

Therefore, in this subsection we consider the case where we retain the condition that the sum of the five phases be a constant, i.e.,

$$\mathbf{t}_5 \cdot \mathbf{x} = C = \text{const} . \tag{2}$$

This permits only a constrained subset of the transformations considered previously in this section. The normal plane is now ($d_\perp = 2$)-dimensional, however, this case turns out to be more complicated than the $4 \rightarrow 2$ case considered in Sec. IV. Still, the permutation properties may be derived in pretty much the same way as in the unconstrained $5 \rightarrow 2$ case. We summarize the results, without repeating the derivations.

Instead of the five-dimensional lattice we now have to consider the slice by the 4-plane. There are now generically five different kinds of "shadow" each of which is a pentagon or an irregular (fivefold symmetric) decagon.[41,42] These are generated by equally spaced layers slicing through the RI normal to its vertical fivefold axis. They start at a height determined by C and are equally spaced along the axis by an amount equal to the separation from one set of RI vertices to the next.

The original Penrose tiling[5]—which we shall call the "proper" Penrose tiling—corresponds to the case $C = integer$, a singular choice of the physical plane which cuts an infinite number of vertices of the 5-cubes. In the proper tiling construction there are only four layers which slice through the vertices as illustrated in Fig. 18(a) of Ref. 20 or Fig. 7 of Ref. 41; there is a symmetry about the midplane so that there are only two kinds of shadow, both pentagons [see Figs. 8 and 9 of Ref. 5; Figs. 18(b) and 18(c) of Ref. 20; Fig. 9 of Ref. 41, or Ref. 42].

The outstanding property of the constrained case is that there are two types of atomic surfaces, which are not equivalent by an symmetry operation. For example, in the "proper" projection construction, a pentagon which is one of the inner two slices of the RI connects along its edges to pentagons from the other inner slice, forming the first type; the second type is formed of pentagons from the adjacent slices, which are patched to each other similarly. [Note that now we just have ten (overlapping) pentagons around each vertex projected on the normal plane, due to the singular choice of C.] In the general "improper" case, all the pentagons become irregular decagons except for those of one of the type 2 slices, and for those of the fifth (and outermost) slice which connect to the decagons from the opposite layer of the type 1.

In the grid language, we can no longer independently move any of the five grids but must always move at least two so as to continue to satisfy (2). We can work out the permutation structure wholly within $d_\perp = 2$ dimensions, reasoning as in the $4 \rightarrow 2$ case (Sec. IV).

In physical space the cubes around a vertex still generate decagons, but now only certain kinds can appear. In the proper Penrose tiling, only those of Fig. 11(a) and 11(f) are allowed. There are nontrivial permutations only in Fig. 11(a). Three of the interior vertices (atoms) belong to each class. Under a small displacement of $x_0^\perp$ *two* of the atoms (one from each class) jump simultaneously. This gives repacking like that in Fig. 7(a)—7(c) without any need for the intermediate state 7(b). The jumps occur simultaneously because of the special singular choice of the physical plane.

The conclusion is that the permutation group of a decagon is isomorphic to the permutation group on three atoms, S_3. Not only is the class conserved, but if we specify the permutation of the class (i) atoms, this forces a corresponding permutation of the class (ii) atoms. We still suspect that the global permutation group consists of all even permutations which preserve the classes, but proving this would be even more problematical than in the unconstrained $5 \rightarrow 2$ case because of the correlations between permutations of the class (i) and class (ii) atoms.

VI. DISCUSSION

We have shown that the imposition of a noncrystallographic symmetry (e.g., a fivefold axis) eliminates the possibility that any atomic surface exists satisfying conditions (1)—(4) of Sec. III. In addition, the smooth atomic surface derived from projection does not satisfy (1)—(4). It may thus seem that we have merely set up an unreasonable criterion and then demolished it. However, the $3 \rightarrow 1$ case does obey (1)—(4), and the Kolmogorov-Arnold-Moser[43] theorem allows one to prove in many cases with $d = 1$ that the atomic surfaces are analytic.

To amplify this last remark, consider, for instance, the Frenkel-Kontorova model[10,11] mentioned in the Introduction:

$$H=\tfrac{1}{2}\sum_n (r_{n+1}-r_n-\rho)^2+\lambda\sum_n \cos(2\pi r_n)\ , \tag{3}$$

where r_n are the atomic positions and ρ is irrational. It expresses the competition between an external potential of period 1 and interatomic springs which prefer an incommensurate spacing ρ. Then for most irrational ρ and λ not too large one can show that the ground state is represented by

$$r_n=\rho n+\chi(\rho n+\phi_0)\ , \tag{4}$$

where χ is an analytic function with period 1, and ϕ_0 is a free phase. With suitable restrictions on λ and ρ to make the atomic surface 1:1 with the normal line, Eq. (4) just represents a line with slope ρ intersecting a periodic family of atomic surfaces labeled by n on a two-dimensional lattice. The intercept of the physical line with the normal line is parametrized by ϕ_0. (This variable is proportional to the $\mathbf{x}_0^\perp$ used above.) The phason degree of freedom in this model just reflects the ability to both assign ϕ_0 arbitrarily, and adjust it continuously. The phason is also a hydrodynamic mode because the energy is independent of ϕ_0 and individual atoms move along well-defined atomic surfaces. These two properties are coupled in this model, since when λ is increased, there comes a point where the atomic surface develops steps and the ground-state energy could depend on ϕ_0. It was anticipated[7,10,27,28] that a similar phenomenon could arise in models of quasicrystals and pin the phasons.

The actual problem seems to us more prosaic. A description of atomic surfaces by conditions (1)—(4) breaks down for purely topological reasons. Thus we see no way to retain both the postulate that $\mathbf{x}_0^\perp$ uniquely determines the atomic positions by fixing the physical plane, and the freedom to adjust $\mathbf{x}_0^\perp$ continuously while maintaining condition 4.

This should be contrasted with Ginzburg-Landau theories of quasicrystals[6–10] which adopt an order parameter that in the icosahedral case is a periodic function of six phases. The incommensurability of the six icosahedral wave vectors guarantees that any reasonable functional of the density will leave the origin of each phase free. While every atomic arrangement appears as a smooth density to x rays, not every density can be written as a smooth form factor centered about a set of atomic sites with reasonable separations. Hence the broken continuous symmetry in the density wave theories is not present in more realistic models involving the actual atoms. (These objections need not apply to an icosahedral state within the blue phase of a cholesteric liquid crystal.[44])

Two whole sections (IV and V) were devoted to examining features (which proved to be unphysical) of the smoothed atomic surface resulting from projection, since we feel that this mode of description may retain some relevance to real systems. For example, the real atomic structures seem to be closely related to the tilings.[45–47]

How do the real quasicrystals evade the consequences of Theorem 2 of Sec. III C? One possibility is to abandon the continuity assumption and an atomic surface description altogether. Another alternative, which appears to have more interesting physical consequences, is to suppose conditions (0) and (1) are violated; that is, there is an element of intrinsic randomness.[26,42,48–51] This in turn suggests the possibility of interesting glassy properties.

Randomness might entail replacement of the atomic surfaces by a smooth probability density in D-space (see Appendix A); however, it can also be realized if there are still atomic surfaces, but with the sites partially occupied in a random fashion, analogous to a lattice gas model. A continuous function could be defined on the surface measuring the probability of an atom; this would not fully describe the model, since there must be correlations between occupancies of nearby sites in order to satisfy the hard-core condition.

An example of this is the random tiling model suggested by Elser.[26,42] In such a case the atomic surfaces continue to be straight normal planes attached to the center of each hypercube, but now, instead of terminating, the patches extend to infinity in the normal space with decaying probability weight. In this case the surfaces would be nonintersecting, but dense.

For another model with randomness, let us assume we have atoms with hard-core interactions in an external (one-body) icosahedral incommensurate potential defined by six phases (one might imagine it as resulting from a charge-density-wave with a large coherence length[52]). As we add atoms to the system, they will occupy local minima of the potential. Note that a locus of local minima defines a 3-surface in six-dimensional space.[20] In this case the surfaces have intersections at branch points.

Near a branch point there will be multiple valleys of the potential, separated by small barriers, and close to each other in physical space so that only one of the valleys may be occupied by an atom. Consequently, these branch points produce double- (or multiple-) well systems of the free energy function in configuration space. Such systems are well known in glasses. They are associated with metastable states, giving rise to slow structural relaxations,[53] through thermal activation over the barriers. They can also be quantum tunneling systems, giving rise to an anomalous low-temperature specific heat.[54]

The above is purely speculation on our part. The general theorem in Sec. III and our entire subsequent discussion has supposed that quasicrystals are "deterministic." In particular, the contents of one cell in the hypercubic lattice plus $\mathbf{x}_0^\perp$ should specify the entire quasicrystal. To specify the state of a random system clearly requires more information.

It should be emphasized that the theorem and the discussion in Sec. III has an important bearing on the distinction between a quasicrystal and an incommensurately modulated crystal. The Frenkel-Kontorova model and the $3\rightarrow 1$ example we considered in Sec. II are the examples of the latter. The generic example is any periodic solid to which we apply a modulation depending on one or more incommensurate vectors. A concrete labeling clearly exists since every atom retains the label it had in the crystal. The first step in our theorem was to show that each type of patch formed a lattice $T_\perp$ and a $d_\perp$-dimensional plane commensurate with the original D-lattice.

We can label these rational planes, and therefore the

atomic surfaces, by forming the quotient $Z^D/T_\perp$. This is just a generalization of the process of modding out by all integer multiples of the basis vectors Γ in Sec. II, and has precisely the same consequences.

It is then very natural to define quasicrystals to be incommensurate systems with δ-function spectra and a noncrystallographic symmetry which forbids a labeling.[55] Incommensurately modulated crystals admit a labeling.

The existence of (unspecified) pathologies of the smoothed projection surface has also been noted by Bak in a recent letter.[18] However, he suggests that alternative atomic surfaces (not derived from projection) exist that would satisfy conditions equivalent to our (0)–(5) of Sec. III, and therefore proposes *deterministic* atomic surfaces on the basis of six-dimensional icosahedral crystallography. What we have shown is that such surfaces do not exist, and therefore the deterministic description is inadequate.

Note added. Spal [Phys. Rev. Lett. **56**, 1823 (1986)] discussed a structure that is topologically equivalent to the example discussed at the end of Sec. III A of our paper. Note that in order to make his structure a "Delaunay system" [i.e., satisfy our Condition (4)], he violates smoothness [our Condition (3)]. He also *conjectures* a theorem similar to our Theorem 1 of Sec. III C.

ACKNOWLEDGMENTS

The authors have had useful conversations with Y. Karpishpan, N. D. Mermin, S. Ostlund, D. Rand, and S. Troian. We are grateful to the National Science Foundation (Grant No. DMR-83-14625) for financial support. D.F. thanks AT&T Bell Laboratories for financial support.

APPENDIX A: *D*-DIMENSIONAL CRYSTALLOGRAPHY

The purpose of this appendix is to motivate the conditions (mentioned in Sec. I and specified in Sec. III) which we demand of our quasicrystal structure; therefore, we do not assume them here. The translational and rotational symmetry, conditions (1) and (5), are inferred from experimental observations. As an example of a six-dimensional space group we describe $P\bar{5}\bar{3}2/m$. The notion of a deterministic quasicrystal [condition (0)] is an idealization which is exactly analogous to the "ideal crystal" traditionally assumed in solid-state physics.

A. Translational periodicity

Experimentally,[1,26] one observes diffraction spots at wave vectors of the following form:

$$\mathbf{q}_{[n]}=\sum_{i=1}^{D} n_i(2\pi/a)\mathbf{u}_i \ , \tag{A1}$$

where the label $[n]$ is a vector $[n_1,\ldots,n_D]$ of D integers and $\mathbf{u}_i$ are D basis vectors (independent over integers); in the experimental icosahedral patterns we have six vectors that point toward the vertices of an icosahedron. Each wave vector $\mathbf{q}_{[n]}$ has a scattering amplitude $F_{[n]}$.[56] Thus, the physical scattering density in real space must be

$$\rho_{\rm phys}(\mathbf{r})=\sum_{[n]} F_{[n]}\exp(i\mathbf{q}_{[n]}\cdot\mathbf{r}) =\rho(\mathbf{x}(\mathbf{r})) \ , \tag{A2}$$

where $\mathbf{r}$ is the 3-space coordinate and $\mathbf{x}$ is a six-dimensional vector with components given by

$$x_i(\mathbf{r})=\mathbf{u}_i\cdot\mathbf{r}/2\pi \tag{A3}$$

and

$$\rho(\mathbf{x})=\sum_{[n]}\exp(2\pi i\mathbf{n}\cdot\mathbf{x}/a) \ . \tag{A4}$$

We can consider (A3) as a parametrization of a d-plane (the "physical plane") cutting through D-space at a special, incommensurate orientation, and (A4) as a periodic density in a D-dimensional cubic lattice with lattice constant a. We can extract d D-dimensional tangent vectors $\mathbf{t}_k$ spanning the physical plane by writing the $\mathbf{u}$ as a $D\times d$ matrix and reading down the columns. Since (A3) represents an incommensurate orientation, it eventually samples every bit of the unit cell; thus no part of the density $\rho(\mathbf{x})$ is superfluous. The same kind of argument can be made for *any* structure with an incommensurate diffraction pattern.[57–59]

The systematic presences and absences of spots in the icosahedral diffraction pattern (the observed pattern is the so-called "vertex pattern"[60,61] indicate that the six-dimensional lattice is the simple cubic, rather than other possibilities such as the six-dimensional fcc, bcc, etc.[7,10,61–63] We have thus determined the translational part of the space group (the "Bravais lattice") for the icosahedral quasicrystals.

B. Space group and point group

Crystallographic space groups include not only the translations (which identify the Bravais lattice) but also operations which include rotations. The set of all rotations which (possibly composed with some translation, as in a glide or screw operation) leave the structure invariant is called the "point group." These rotations must preserve the Bravais lattice; in terms of its basis vectors, the point group must consist of matrices of integers with determinant ±1. Furthermore, for our structures, defined by lower-dimensional cuts, the higher-dimensional point group must take the physical and normal subspaces into themselves without any mixing.[22,60,61,62]

Incommensurately modulated crystals provide a relatively trivial example of the above.[13] In this case, the D-dimensional Bravais lattice is a direct sum of an ordinary d-dimensional lattice and a $d_\perp$-dimensional lattice. The action of the D-dimensional point group on the physical plane is just that of the d-dimensional point group of the unmodulated crystal. The possible space groups have been classified.[57–59]

In general, the point group must be a symmetry of the "holohedral group"[64] which contains all symmetry operations preserving the D-dimensional Bravais lattice. Also, if the point group were contained in the homohedral group of some less symmetric Bravais lattice, there is no symmetry reason to prevent the (quasi)crystal from distorting to the less symmetric lattice. Consequently, the

observed symmetry of spot positions indicates a certain minimum point group symmetry; for the icosahedral quasicrystal case, an icosahedral point group. Convergent-beam electron diffraction confirms that the point group of quasicrystalline Al-Mn [Ref. 65(a)] and Al-Li-Cu-Mg [Ref. 65(b)] is the 120-element icosahedral group including mirror planes, known as "$\bar{5}\bar{3}2/m$."

C. The space group $P\bar{5}\bar{3}2/m$

There are several six-dimensional space groups with the simple cubic Bravais lattice and the icosahedral point group $\bar{5}\bar{3}2/m$. The icosahedral space groups may be classified[62,63,66] as in the 3D case. The strict-projection structure corresponds to one of these, called "$P\bar{5}\bar{3}2/m$" (extending the standard Hermann-Mauguin notation for space groups[64]). This is also the space group of the structure produced by placing atoms on local maxima of density waves[67] (in physical space); thus it is reasonable to assume that $P\bar{5}\bar{3}2/m$ is the correct symmetry group of the icosahedral crystals.

In $P\bar{5}\bar{3}2/m$, the icosahedral operations are represented by matrices of ones and zeroes. The fivefold rotation leaving projections of the axis $\mathbf{e}_1$ into normal and physical space, $\mathbf{e}_1^{\perp}$ and $\mathbf{e}_1^{\parallel}$, invariant is[37]

$$\begin{bmatrix} 1 & 0 & 0 & 0 & 0 & 0 \\ 0 & 0 & 1 & 0 & 0 & 0 \\ 0 & 0 & 0 & 1 & 0 & 0 \\ 0 & 0 & 0 & 0 & 1 & 0 \\ 0 & 0 & 0 & 0 & 0 & 1 \\ 0 & 1 & 0 & 0 & 0 & 0 \end{bmatrix}, \tag{A5}$$

the threefold rotation around an axis leaving $\mathbf{e}_1^{\perp}+\mathbf{e}_2^{\perp}+\mathbf{e}_3^{\perp}$ and $\mathbf{e}_1^{\parallel}+\mathbf{e}_2^{\parallel}+\mathbf{e}_3^{\parallel}$ invariant is

$$\begin{bmatrix} 0 & 1 & 0 & 0 & 0 & 0 \\ 0 & 0 & 1 & 0 & 0 & 0 \\ 1 & 0 & 0 & 0 & 0 & 0 \\ 0 & 0 & 0 & 0 & 0 & 1 \\ 0 & 0 & 0 & -1 & 0 & 0 \\ 0 & 0 & 0 & 0 & -1 & 0 \end{bmatrix}, \tag{A6}$$

and the mirror reflection in the 4-plane containing $\mathbf{e}_1^{\perp}$, $\mathbf{e}_2^{\perp}$, $\mathbf{e}_1^{\parallel}$, and $\mathbf{e}_2^{\parallel}$ is

$$\begin{bmatrix} 1 & 0 & 0 & 0 & 0 & 0 \\ 0 & 1 & 0 & 0 & 0 & 0 \\ 0 & 0 & 0 & 0 & 0 & 1 \\ 0 & 0 & 0 & 0 & 1 & 0 \\ 0 & 0 & 0 & 1 & 0 & 0 \\ 0 & 0 & 1 & 0 & 0 & 0 \end{bmatrix}. \tag{A7}$$

These operations suffice to generate the group. They all act at a point. Both [0,0,0,0,0,0] and $[\frac{1}{2},\frac{1}{2},\ldots,\frac{1}{2}]$ type points posses this symmetry, but they are not equivalent. (For example, in the projection structure discussed in Sec. V the latter points are the ones projected, while the former ones are associated with the jumps and other pathologies.) This space group has an inversion center.

D. Perfect crystals and quasicrystals

We have not yet specified the nature of the density $\rho(\mathbf{x})$ [and hence $\rho_{\text{phys}}(\mathbf{r})$]. We may imagine each atom as being a point scatterer. (For the physical diffraction pattern, we just convolve these with the density profiles of the real atoms' electron clouds.)

In ordinary d-dimensional crystals, a perfect crystal means one in which the position (and chemical identity) of each atom is determined, if we have fixed the location of one unit cell. Then $\rho_{\text{phys}}(\mathbf{r})$ is just a sum of δ functions in a periodic array, each with a weight of one atom. However, we may also have disordered crystals, e.g., with random vacancies or displacements. In this case, the Bragg part of the scattering is the Fourier transform of an averaged density which is still periodic may be constructed by folding all unit cells back into one representative one which is repeated. There might still be δ functions with fractional weights, or these might be smeared into a continuous density.

What is the natural generalization of "perfect crystals" for quasicrystals? We require that the physical density consist of δ functions with unit weight. It follows that the D-dimensional density locally has the form

$$\rho(\mathbf{x})=\delta(\mathbf{x}^{\parallel}-\boldsymbol{\phi}(\mathbf{x}^{\perp}))\ , \tag{A8}$$

where $\boldsymbol{\phi}$ is a d-vector function of a $d_{\perp}$-vector argument, $(d_{\perp}=D-d)$. Globally this defines a set of d-dimensional hypersurfaces which are repeated periodically in D-dimensional space; this is that we call a deterministic quasicrystal.

An example of this is the "Kolmogorov-Arnold-Moser (KAM) surface" of the Frenkel-Kontorova model: Eq. (4) in Sec. VI is equivalent to (A8) by the implicit function theorem. A more general case in which (A8) has been is for incommensurately modulated crystals, e.g., the case $d=d_{\perp}=2$ for incommensurate adsorbed monolayers on a triangular substrate.[11]

APPENDIX B: PARTITIONS OF D-SPACE BY HYPERPLANES

Suppose we have n $(d-1)$-dimensional hyperplanes in a d-dimensional space. We assume that the choice of hyperplanes is generic. They break up the space into bounded and unbounded regions. Let B_n^d and U_n^d be the numbers of bounded and unbounded regions, respectively. The purpose of this appendix is to derive general formulas for U_n^d and B_n^d. Formulas (B3) and (B8) contain our results.

To do so, we set up recurrence relations. Suppose we know U_n^d and B_n^d. Add one more $(d-1)$-dimensional hyperplane. It will intersect each of the other hyperplanes along a $(d-2)$-dimensional plane. We thus cut out n $(d-2)$-planes in the new $(d-1)$-hyperplane, which break up into B_n^{d-1} and U_n^{d-1} bounded and unbounded regions, respectively. Each of the $(d-1)$-dimensional pieces in the new hyperplane breaks up one of the regions in the original space into two. In particular, each of the bounded $(d-1)$-dimensional regions means a creation of a new d-dimensional bounded region, and each unbounded piece of the new hyperplane means a new unbounded d-

dimensional region. So,

$$U^d_{n+1}=U^d_n+U^{d-1}_n,\quad B^d_{n+1}=B^d_n+B^{d-1}_n\ . \tag{B1}$$

To solve these equations we need initial conditions. We know that at least $(d+1)$ hyperplanes are needed in a d-dimensional space to bound a region. Thus,

$$B^d_n=0,\quad n\le d,\quad B^d_{d+1}=1\ . \tag{B2}$$

It is easy to see that

$$\begin{aligned} &B^d_n=0,\quad n\le d\ ,\\ &B^d_n=\begin{bmatrix} n-1 \\ d \end{bmatrix}=\frac{(n-1+d)!}{d!(n-1)!},\quad n>d \end{aligned} \tag{B3}$$

solve both the initial condition (B2) and the recurrence relations for B^d_n due to the known relations among the binomial coefficients:

$$\begin{bmatrix} n+1 \\ d \end{bmatrix}=\begin{bmatrix} n \\ d \end{bmatrix}+\begin{bmatrix} n \\ d-1 \end{bmatrix},\quad \begin{bmatrix} d \\ d \end{bmatrix}=1\ . \tag{B4}$$

To complete the proof that (B3) is the correct solution, we check it for all n at some particular value of d. If $d=1$, we have n points on a line which lead to $(n-1)$ bounded regions. From (B3), $B^{d=1}_n=(n-1)$, as needed.

Deriving U^d_n is not so straightforward due to a different initial condition, which is

$$U^d_n=2^n,\quad n\le d\ . \tag{B5}$$

In fact, an expression for U^d_n is most easily found using

$$U^d_n=U^{d-1}_n+2B^{d-1}_n\ . \tag{B6}$$

This relation can be obtained from the following geometric considerations. Unbounded regions cannot be created or destroyed when we displace one of the hyperplanes a finite distance without changing its orientation in space. So, we can shift all n hyperplanes until they all pass through one point, and there are still U^d_n unbounded sectors.

Draw a $(d-1)$-dimensional sphere centered at that point. Each hyperplane intersects this sphere along a $(d-2)$-dimensional "great circle." The number of [$(d-1)$-dimensional] regions into which these n great circles divide the sphere is exactly U^d_n. We can choose these great circles in such a way that their intersections lie in two restricted areas surrounding the two poles [see Fig. 10(a), which illustrates $d=3$, $n=4$ case]. Now, in the neighborhood of each pole the sphere looks flat, and is broken up by parts of these great circles, which look like straight lines in this small area, into "bounded" and "unbounded" regions [Fig. 5(b)].

The identical bounded regions appear on the other side of the sphere. What looks like unbounded regions locally are just regions which are not localized at one of the poles, but rather extend all the way across the sphere from one pole to another. Since locally at the poles it looks like a $(d-1)$-dimensional space [Fig. 5(b)] broken up by n $(d-2)$-dimensional lines, we have thus the total number of regions on the sphere given by

$$U^{d-1}_n+2B^{d-1}_n\ . \tag{B7}$$

This, however, was shown to be equal to U^d_n. Hence we get (B4).

Iterating (B4) several times we get

$$\begin{aligned} U^d_n&=2(B^{d-1}_n+B^{d-2}_n+\cdots+B^1_n+1)\\ &=2\left[\begin{bmatrix} n-1 \\ d-1 \end{bmatrix}+\begin{bmatrix} n-1 \\ d-2 \end{bmatrix}+\cdots+\begin{bmatrix} n-1 \\ 1 \end{bmatrix}+1\right]. \end{aligned} \tag{B8}$$

For $n=d$, we get $U^d_{n=d}=2^d$ by a known identity, which satisfies the required boundary condition. It is also easy to check directly that (B8) satisfies the recursion relation (B1) for U^d_n.

To show (B8) is a unique solution, we check, just like for B^d_n, that we get correct results for $d=1$. N points on a line create only two unbounded regions. So, we expect $U^1_n=2$ for $n\ge 1$. Indeed, (B8) gives,

$$U^1_n=2\times[1]=2,\quad n\ge 1\ . \tag{B9}$$

APPENDIX C: DETAILS OF COMPUTING PERMUTATIONS AT A VERTEX

In this appendix we explicitly show how to construct the group of permutations of "atoms" induced by small movements of the physical plane around a single vertex in the case of the 5→2 projection. Recall from the text that the unstable 5-cubes at a vertex project onto 22 rhombic icosahedra (RI). Those of their faces which contain a common vertex may be reassembled into ten planes which divide up a sphere around that point into 62 regions. The top view of that sphere is shown in Fig. 13.

We now have to learn to identify intersections of a single RI with that sphere. (We called this a spherical polygon.) To within different orientations all possible kinds of spherical polygons obtained that way are depicted in Figs. 14(a)–14(c).

As explained in Sec. V, various loops on the surface of that sphere depict various motions of the physical plane normal to itself. Nontrivial permutations arise when a loop encircles one or more of the points where four great circles meet. Consider a loop that encircles exactly one of them (Fig. 15). The region marked with × on Fig. 15 is

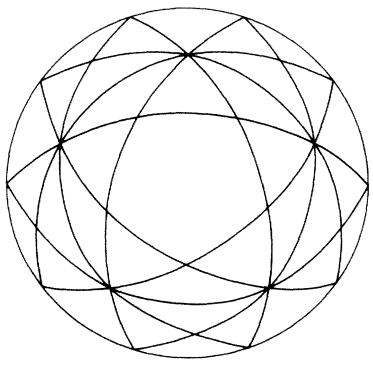

FIG. 13. Intersections of 22 rhombic icosahedra (RI) sharing a vertex with a small sphere around the vertex creates ten great circles which are shown here. These RI are projections of the 22 "unstable" cubes into normal plane.

covered by exactly six spherical polygons. One of them, number 1, is shown in Fig. 14(a); the rest, numbers 2–6, are shown in Fig. 15, where the numbered arrows identify the boundaries and point toward the interior of various polygons. It is clear from Fig. 15 that polygons 4–6 cover the ×-marked region as well as the loop drawn around the vertex; thus the atoms projected from the corresponding 5-cubes do not permute. On the contrary, the loop crosses the boundaries of polygons 1–3, so their atoms

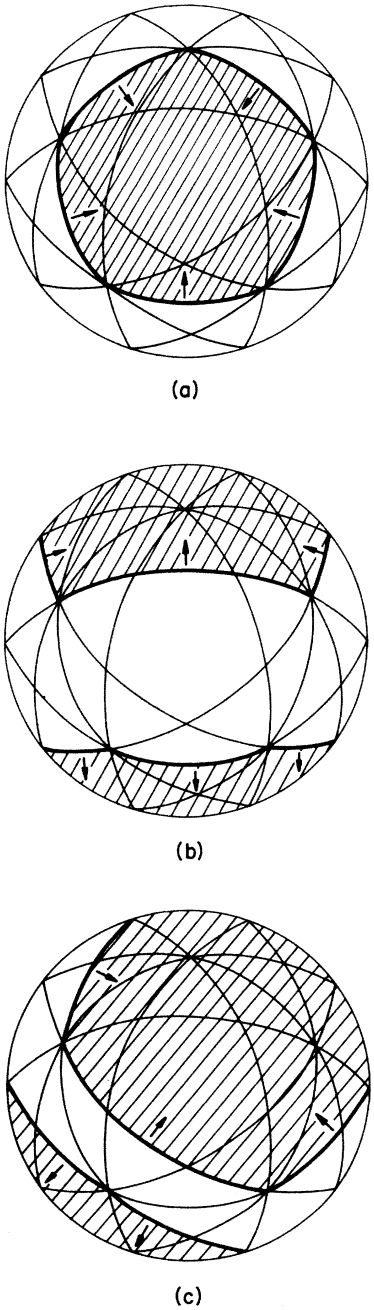

FIG. 14. On the three figure here we show (up to orientation) all possible "spherical polygons," objects formed by intersection of a single rhombic icosahedron with a sphere. Arrows, as well as the shading, indicate the interior of the spherical polygon.

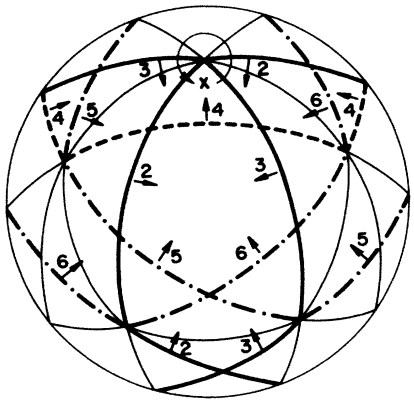

FIG. 15. Here we show the six spherical polygons that cover the ×-mark regions. Polygon 1 is as in Fig. 14(a). Numbered arrows point toward the interior of polygons 2–6 (compare with Fig. 14). Dashed and dash-dotted lines also help in identifying the boundaries of various polygons. Polygons 1–3 will permute under the action of the indicated loop (see also Fig. 16).

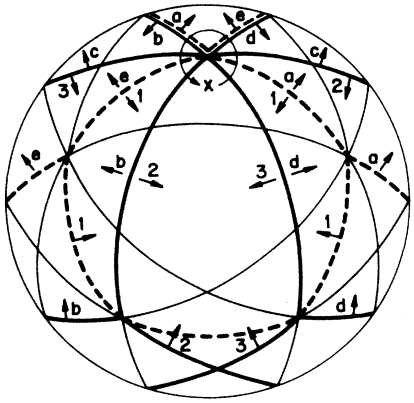

FIG. 16. Permutations induced by a small loop around a vertex. As we move around the loop we may go through a number of intermediate spherical polygons, which are denoted by letters a–e.

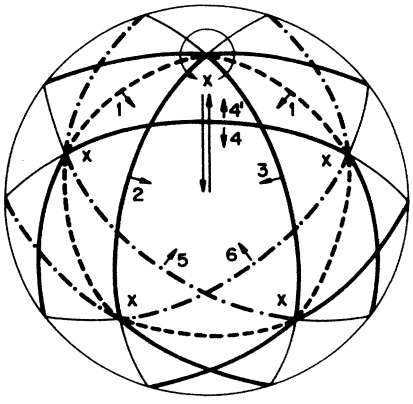

FIG. 17. Six polygons covering the central region as shown. They permute under the action of various loops. The generators are obtained by moving from the center to one of the x-marked regions, looping around the corresponding vertex, and then going back to the starting point.

may undergo a permutation. In Fig. 16 we show only those polygons that can be reached by a loop on a multisheeted polygonal covering of the sphere which starts from one of the polygons 1—3 and remains in the vicinity of $\times$. Clearly, only these polygons are needed to ascertain the permutation induced by closed loop on (1—3). The remainder of the arrangement is now very similar to the $4\rightarrow 2$ case, described in Sec. IV.

When we move along the loop from $\times$, we first reach the common boundary of polygons 1 and a. As we keep moving along the loop, we eventually reach a common boundary of a and b; and finally we return from b to 2, where we stop. This path is denoted as $1\rightarrow a\rightarrow b\rightarrow 2$, so an atom in cube 1 moves continuously into an atom in cube 2. Similarly, we have paths $2\rightarrow c\rightarrow 3$ and $3\rightarrow d\rightarrow e\rightarrow 1$. All in all we have $1\rightarrow 2$, $2\rightarrow 3$, $3\rightarrow 1$, which means our loop induces a 3-cycle (123), which is an element of the group of permutations of six objects S_6.

There are altogether ten such vertices on the sphere (five are visible in our figures). Each of them corresponds to a 3-cycle. We are interested, however, in the group of permutations due those loops that *all* start and end in one single region. It is easist to use the central "pentagonal" regions as a base for all our loops (Fig. 17). We then get all the group generators by connecting it to any of the "peripheral" $\times$-marked regions by a path as shown in Fig. 17.

The six polygons covering the central region are shown in Fig. 17. To get from the central to a peripheral $\times$-marked region, our path only crosses the boundary of spherical polygon 4, and enters polygon 4′. Then, a loop around the vertex induces a permutation on (1,2,3), as shown above. On the return path 4′ returns to 4, which commutes with the permutation (123) and thereby cancels $4\rightarrow 4'$. Thus the permutations is induced only among 1, 2, and 3, which are just those of the six spherical polygons that meet at the fourfold vertex the small loop was drawn about.

We can check that the triples of polygons that meet at the other four vertices on the depicted half of the sphere are (146), (135), (126), and (145). Together with (123), they define the 3-cycles that are the generators of the group.

To get the other five vertices we would have to draw an open path to the other side of the sphere. While it is not very hard, we do not need to do it. Each of those extra permutations would also be a 3-cycle. However, all 3-cycles are even permutations, and we can show that the five 3-cycles we have already obtained generate all even permutations of six objects. Showing it is entirely trivial, and we do not reproduce the manipulations.

[1]D. Shechtman, I. Blech, D. Gratias, and J. W. Cahn, Phys. Rev. Lett. **53**, 1951 (1984).

[2]L. Bendersky. Phys. Rev. Lett. **55**, 1461 (1985).

[3]D. Levine and P. J. Steinhardt, Phys. Rev. Lett. **53**, 2477 (1984).

[4]D. Levine and P. J. Steinhardt, Phys. Rev. B **34**, 596 (1986).

[5]N. G. de Bruijn, Proc. Konink. Ned. Akad. Wetensch. A **84**, 39 (1981); **84**, 53 (1981) (see I, Figs 8 and 9).

[6]P. A. Kalugin, A. Yu. Kitaev, and L. S. Levitov, Pis'ma Zh. Eksp. Teor. Fiz. **41**, 119 (1985) [JETP Lett. **41**, 145 (1985)].

[7]P. A. Kalugin, A. Yu. Kitayev, and L. S. Levitov, J. Phys. (Paris) Lett. **46**, L-601 (1985).

[8]N. D. Mermin and S. M. Troian, Phys. Rev. Lett. **54**, 1524 (1985).

[9]P. Bak, Phys. Rev. Lett. **54**, 1517 (1985).

[10]P. Bak, Phys. Rev. B **32**, 5764 (1985).

[11]V. L. Pokrovsky and A. L. Talapov, *Theory of Incommensurate Crystals* (Harwood Academic, New York, 1984), Sec. 4.7.

[12]P. Bak. Rep. Prog. Phys. **45**, 587 (1981).

[13]P. M. de Wolff, Acta Crystallogr. Sect. A **30**, 777 (1974).

[14]A. Janner and T. Janssen, Phys. Rev. B **15**, 643 (1977).

[15]M. Peyrard and S. Aubry, J. Phys. C **16**, 1593 (1983).

[16]P. Bak, in *Scaling Phenomena in Disordered Systems*, edited by R. Pynn and A. Skjeltorp (Plenum, New York, 1986), p. 197.

[17]P. Bak (unpublished).

[18]P. Bak, Phys. Rev. Lett. **56**, 861 (1986).

[19]C. L. Henley, J. Non-Cryst. Solids **75**, 91 (1985).

[20]C. L. Henley, Phys. Rev. B **34**, 797 (1986).

[21]D. Rand (personal communication).

[22]P. Kramer and R. Neri, Acta Crystallogr. Sect. A **40**, 580 (1984).

[23]M. Duneau and A. Katz, Phys. Rev. Lett. **54**, 2688 (1985).

[24](a) A. Katz and M. Duneau, J. Phys. (Paris), Colloq. **46**, C8-31 (1985); (b) J. Phys. (Paris) **47**, 181 (1986).

[25]V. Elser, Acta Crystallogr. Sect. A **42**, 36 (1986).

[26]V. Elser, Phys. Rev. B **32**, 4892 (1985).

[27]D. Levine, T. C. Lubensky, S. Ostlund, S. Ramaswamy, P. J. Steinhardt, and J. Toner, Phys. Rev. Lett. **54**, 1520 (1985).

[28]T. C. Lubensky, S. Ramaswamy, and J. Toner, Phys. Rev. B **32**, 7444 (1985).

[29]References 23—26 projected vertices; the result here is the same since the centers of cubes form a lattice equivalent to that of the vertices.

[30]This shadow is an example of a "*zonogon*," a polygon whose interior consists of all convex combinations of a discrete set of basis vectors. The octagons of Sec. IV are also zonogons. In three dimensions, we analogously define "zonohedra"; the rhombic icosahedron and triacontahedron of Sec. V are examples. Note that the faces of a zonohedron are all parallelograms; also, zonogons and zonohedra always have inversion symmetry.

[31]Take a tiling constructed by projection and place an atom at the center of each tile; this defines a stepped atomic surface which are projections from the $d_\perp$-faces of the D-cubes. If we smooth out these atomic surfaces, we get the family of hypersurfaces described in this example. Although they have intersections, the atoms do *not* permute under loops of $x_0^\perp$, and so labeling is possible.

[32]The idea that crystallographic symmetry restricts the possible arrangement of surfaces was first spelled out by Bak (Refs. 16—18). He did not, however, explore the relation between the existence of continuous movements of atoms and noncrystallographic symmetry, and he does not state that they are in-

compatible with one another.

[33]Conceivably the operation acts trivially in the d-dimensional subspace. If so, it acts nontrivially in the $d_\perp$-dimensional quotient space which (if $d_\perp \geq D/2$ as assumed in Sec. III B), satisfies $d_\perp \leq d$.

[34]The singular objects, such that paths of $\mathbf{x}_0^\perp$ around them in $\mathbf{x}^\perp$ space generate nontrivial permutations, are of course topological defects; their dimension is in general $d_\perp - 2$. See N. D. Mermin, Rev. Mod. Phys. **51**, 591 (1979), for an introduction to topological defects in condensed-matter physics.

[35]J. E. S. Socolar, P. J. Steinhardt, and D. Levine, Phys. Rev. B **32**, 5547 (1985).

[36]F. Gähler and J. Rhyner, J. Phys. A **19**, 267 (1986).

[37]We use the conventions of Refs. 25 and 26 for the choice of the physical plane and the numbering of the axes.

[38]Note also that in the 2D Penrose tiling every vertex of a rhombus belongs to at least one decagon.

[39]In the 6→3 case the elementary rearrangements analogous to Fig. 8 are repackings of rhombic dodecahedra (RD; see, for example, Ref. 20, Fig. 15); these are zonohedra projected from 4-faces. Each RD is composed of four rhombohedra of the three-dimensional Penrose tiling, packed together. There is one internal vertex and only it moves in the repacking. Note that if we label the tiling vertices alternately "even," "odd,"..., then the interior vertex of the RD can be seen to jump to a site of the same parity; this is an alternative way to see the even/odd conservation stated in Theorem 3. In 2D, there is no such conservation since the interior vertex in a hexagon jumps to a site of opposite parity. Just as the decagons of the 5→2 case are packed with 10 rhombi (recall Fig. 11), the triacontahedron is packed with 20 rhombohedra, ten of the prolate and ten of the oblate type. Such a packing is depicted by a stereogram in Fig. 8 of A. L. Mackay, Sov. Phys. Crystallogr. **26**, 517 (1981) [Kristallografiya **26**, 910 (1981)]. However, not every possible packing can be generated by projection—in fact only one can. We can build up the packing as follows. We will orient the triacontahedron in a cubic fashion, so that x, y, and z axes are twofold axes. First we place an RD on its broad side; its bottom five faces are exterior faces of the triacontahedron. Over the topmost face of this RD we place another RD, with its long axis perpendicular to that of the first. [Note that RD's related in this fashion may be seen in Fig. 4(a) of Ref. 46.] The top face of the second RD is the top of the triacontahedron, but all the other faces are interior. From the bottom up, we add two oblate rhombohedra (at top and bottom, touching the lengthwise faces of the bottom RD); four prolate rhombohedra; two more prolate rhombohedra (on the right and left sides); four more oblate rhombohedra (around the top face, forming the upper surface of the triacontahedron). Apart from the way the RD's are broken up into rhombohedra (which is arbitrary), the arrangement has a 2×2 symmetry around the vertical axis. There are ten internal sites—three of one parity and seven of the other—which is another way of seeing why the permutation group of the triacontahedron is a subgroup of $S_3 \otimes S_7$.

[40]Note that in the 5→2 case we could obtain *all* tilings of a decagon as a projection of six unstable cubes. In the 6→3 case we do not get all of the tilings of a triacontahedron that way.

[41]M. V. Jarić, Phys. Rev. B (to be published).

[42]D. P. DiVincenzo, Proceedings of the Les Houches Workshop on Aperiodic Crystals [J. Phys. (Paris) Colloq. **47**, C3-237 (1986)].

[43]See J. Moser, *Stable and Random Motions in Dynamical Systems* (Princeton University Press, Princeton, New Jersey, 1973).

[44]R. M. Hornreich and S. Shtrikman, Phys. Rev. Lett. **56**, 1723 (1986); D. S. Rokhsar and J. P. Sethna, *ibid.* **56**, 1727 (1986).

[45]P. Guyot and M. Audier, Philos. Mag. B **52**, L15 (1985). M. Audier and P. Guyot, *ibid.* B **53**, L43 (1986).

[46]V. Elser and C. L. Henley, Phys. Rev. Lett. **55**, 2883 (1985).

[47]C. L. Henley and V. Elser, Philos. Mag. B **53**, L59 (1986).

[48]The topological constraints we have uncovered might be considered a form of "frustration" peculiar to quasicrystals, which prevents attainment of a deterministic structure in a realistic model. See, for example, M. Kléman and J. F. Sadoc, J. Phys. (Paris) Lett. **40**, L569 (1979); D. R. Nelson, Phys. Rev. B **28**, 5515 (1983).

[49](a) V. Elser, Phys. Rev. Lett. **54**, 1730 (1985); (b) T. C. Lubensky, J. E. S. Socolar, P. J. Steinhardt, and P. A. Heiney (unpublished); (c) P. M. Horn, W. Malzfeldt, D. P. DiVincenzo, J. Toner, and R. Gambino (unpublished).

[50]P. W. Stephens and A. I. Goldman, Phys. Rev. Lett. **56**, 1168 (1986).

[51]S. Sachdev and D. R. Nelson, Phys. Rev. B **32**, 4592 (1985).

[52]J. P. Straley (unpublished); E. D. Siggia (unpublished).

[53]H. S. Chen and C. H. Chen, Phys. Rev. B **33**, 668 (1986).

[54]P. W. Anderson, B. I. Halperin, and C. M. Varma, Philos. Mag. **25**, 1 (1972).

[55]This generalizes the definition of quasicrystal in Ref. 4.

[56]Experimentally, only the magnitudes $|F_{[n]}|$ are measured. We shall not discuss the crystallographic problem of determining the phases.

[57]P. M. de Wolff, Acta Crystallogr. Sect. A **33**, 493 (1977).

[58]A. Janner and T. Janssen, Acta Crystallogr. Sect. A **36**, 399 (1980).

[59]A. Janner, T. Janssen, and P. M. de Wolff, Acta Crystallogr. Sect. A **39**, 658 (1983).

[60]D. R. Nelson and S. Sachdev, Phys. Rev. B **32**, 689 (1985).

[61]J. W. Cahn, D. Shechtman, and D. Gratias, J. Mater. Res. **1**, 13 (1986).

[62]S. Alexander, Proceedings of the Les Houches Workshop on Aperiodic Crystals [J. Phys. (Paris) Colloq. **47**, C3-143 (1986)].

[63]T. Janssen, Proceedings of the Les Houches Workshop on Aperiodic Crystals [J. Phys. (Paris) Colloq. **47**, C3-85 (1986)]; T. Janssen, Acta Crystallogr. Sect. A **42**, 261 (1986).

[64]*International Tables for Crystallography,* edited by Theo Hahn (Riedel, Dordrecht/Boson, 1983), Vol. A.

[65](a) L. A. Bendersky and M. J. Kaufman, Philos. Mag. B **53**, L75 (1986); (b) W. A. Cassada, G. J. Shiflet, and S. J. Poon, Phys. Rev. Lett. **56**, 2276 (1986).

[66]D. Wright and D. Rokhsar (personal communication).

[67]See Ref. 20, Appendix C, and references therein.